HIGHWAY RESEARCH RECORD

Number 346

Design of Sign Supports and Structures

6 Reports

Subject Areas

22 Highway Design
51 Highway Safety

HIGHWAY RESEARCH BOARD

DIVISION OF ENGINEERING NATIONAL RESEARCH COUNCIL
NATIONAL ACADEMY OF SCIENCES—NATIONAL ACADEMY OF ENGINEERING

WASHINGTON, D. C. 1971

ISBN 0-309-01957-5

Price: $2.40

Available from

Highway Research Board
National Academy of Sciences
2101 Constitution Avenue
Washington, D.C. 20418

GROUP 2—DESIGN AND CONSTRUCTION OF TRANSPORTATION FACILITIES

John L. Beaton, California Division of Highways, Sacramento, chairman

SECTION A—GENERAL DESIGN

F. A. Thorstenson, Minnesota Department of Highways, St. Paul, chairman
Lawrence F. Spaine, Highway Research Board staff

Committee 4—Traffic Safety Barriers and Sign, Signal and Lighting Supports

Eric F. Nordlin, California Division of Highways, Sacramento, chairman
Verdi Adam, W. C. Anderson, William C. Burnett, Edward M. Conover, James J. Crowley, Albert L. Godfrey, Sr., Malcolm D. Graham, Alf H. Hansen, Wayne Henneberger, Robert N. Hunter, Jack E. Leisch, Edwin C. Lokken, Jarvis D. Michie, Gilbert E. Morris, Jr., Robert M. Olson, John M. Quigg, Edmund R. Ricker, Neilon J. Rowan, Frank G. Schlosser, Paul C. Skeels, Flory J. Tamanini, James A. Thompson, Charles Y. Warner, M. A. Warnes, Earl C. Williams

FOREWORD

The primary purpose for highway furniture, such as signs, signals, and luminaires, is to guide and protect the traveling motorist. However, the supports for these same roadside appurtenances can be hazards and sometimes lethal fixed objects for errant vehicles leaving the roadway. In recent years, highway design engineers have minimized this accident problem by placing these supports at safer distances from the traveled way, by making them yielding or breakaway and, as a last resort, by erecting properly designed traffic safety barriers to protect the motorist from impact into them. Overhead signs have offered the most difficult problem because their structures must span the roadway and their supports must bear the greater dead and wind loads imposed on them. The six papers in this RECORD deal with the design and testing of sign structures and supports, including design criteria and features aimed at improving the safety aspects of overhead sign supports.

In the first paper, Pelkey examines the current AASHO specifications for allowable dead-load deflections in overhead sign structures. He concludes that more liberal dead-load deflections are permissible for long-span monotubular structures. The paper reports on the design, construction, and excellent 2-3 year service performance of several such structures involving spans up to 156 ft and single large-diameter, thin-walled pipe members. Designs for monotubular structures have been completed for spans up to 200 ft in length.

The second paper examines the present AASHO critical buckling stress requirements and concludes that rigorous adherence to them can result in the design of heavier supports for overhead sign structures than are necessary. Gunderson, Cetiner, and Olson develop and propose a less conservative buckling stress formula that is shown to be consistent with available test results. If buckling stress is the limiting factor in the design, the use of the proposed formula could result in significant savings in support material. This is of particular importance in the design of breakaway supports where the mass must be kept to a minimum to reduce damage to impacting vehicles and injury to passengers.

Martinez, Olson, and Post report on the general design considerations and the results of the mathematical simulation of vehicle collisions with overhead sign structures mounted on breakaway supports. The results were verified by observations of seven full-scale crash tests into a prototype design. The authors conclude that the application of the breakaway concept to the supports of an overhead sign structure is feasible. The prototype structure is shown to possess the ability to withstand the torsional loads imparted to it by the rotating breakaway support and still remain stable under the impact forces.

The paper by Olson, Ivey, Buth, Hirsch, and Hawkins complements the previous paper by describing the results of and evaluating the behavior of nine head-on and 15-degree-angle passenger car crash tests

at speeds up to 75 mph into the prototype overhead sign structure with breakaway supports. The authors conclude that the safety features of the prototype structure will operate adequately to greatly reduce the forces on impacting vehicles. Also, that the prototype structure, as modified with steel-tube impact attenuators, can successfully sustain high-speed, 5,000-lb passenger-car impacts at angles up to 15 degrees without severe structural damage.

Ross presents the results of a series of wind-tunnel tests of both straight and curved louvered sign models. He concludes that reductions of approximately 50 percent in wind loads can be realized by the use of louvered signs as compared to conventional flat solid-surface signs. Such a reduction in wind loads could result in more economical long-span overhead sign structures and a reduction in the size of roadside and overhead sign supports, thereby reducing the hazard to the motorists. This paper provides a concise and convenient source of information for determining wind loads on louvered signs.

Cook and Bodocsi report on an investigation of yielding lightweight steel "hat-section" supports for small and intermediate-size roadside signs. This study included laboratory testing on a crash simulator, computer programming to simulate and extrapolate the results, and 40 vehicle impact tests with velocity, angle-of-collision, sign type, and soil-support conditions as variables. The authors conclude that the lightweight steel sign supports they investigated will yield safely under impact with vehicle deceleration values well below human tolerance levels. Both single- and double-post signs were investigated.

—Eric F. Nordlin

CONTENTS

NEW DESIGN APPROACH TO LONG-SPAN OVERHEAD SIGN STRUCTURES

Ron E. Pelkey, De Leuw, Cather and Company of Canada Ltd.

The use of long-span sign structures of improved appearance is required to meet the higher safety and alignment standards for modern highways. Current specifications impose restrictive limitations on allowable dead-load deflections for such structures. The basis for these limitations involves the assumption that both the fundamental frequency of vibration of the structure and the frequency of vortex shedding are in harmony at a design wind speed of 80 mph.

A study was conducted to examine this assumption. The results show that it does not hold for the basic equations applying specific parameters from actual structural designs. An analogy is made with roadway lighting poles. A deflection-limiting relationship developed on the same basis as that developed from the current specifications shows that standard light-gage steel poles, as we know them, would not have been developed had such a limit on their deflection been required. Therefore, a consistent philosophy with respect to the design of both roadway lighting poles and overhead sign structures is desirable.

As a part of this study, designs for monotubular structures have been completed for clear spans up to 200 ft, sufficient to span 10 lanes of divided traffic with adequate safe outside shoulder clearance and capable of supporting as many as four full-size freeway signs. Also, several such structures involving spans as long as 156 feet have been built and have been in service for 2 to 3 years. The performance of these structures in winds of gust speeds as high as 65 mph has been excellent. It is concluded that more liberal allowable dead-load deflections are permissible for this type of structure. This new freedom in design makes possible simple, efficient, safe, and attractive long-span highway sign structures.

A GREAT deal of progress has been made in recent years in improving safety features and aesthetic standards of modern highways. On controlled-access highways in particular, higher standards are being applied to geometric design and cross-sectional features. Research has been extended into almost every area that has application to highway engineering. The results have been impressive. Much work remains to be done, however.

The development of long-span sign structures to meet new safety and aesthetic standards has received little attention until recently. In an attempt to overcome this situation this study has been carried out to examine present design criteria and to explore possibilities for developing new types of long-span sign structures. The study revealed that deflection limitations set by existing design specifications (1) represent a most severe restraint on the selection of structural types and on the creation of aesthetic designs.

As a result of the study several long-span designs were evolved utilizing hollow thin-walled single tubular members. Designs have been completed for spans ranging up to 200 ft in length. Several have been built including spans as long as 156 ft. The shape of the sign structure was chosen to complement that of the single-davit curved light

Sponsored by Committee on Traffic Safety Barriers and Sign, Signal and Lighting Supports and presented at the 50th Annual Meeting.

poles used. Both poles and sign structure support columns are located at the same offset dimension from the edge of pavement. Both are finished in the same color of field paint. The result is seen as a simple, efficient, safe, and attractive highway sign structure. Symbols used in this paper are listed in an appendix.

CONSIDERATION OF SIMPLICITY, SAFETY, AND AESTHETICS

The need for overhead sign supports has been met in the past by the development of three-dimensional truss spans and frames. These have been made up of small member aluminum or steel angles, channels, plates, and tubes. Figure 1 shows an example of this type of installation. A column support has been located in the gore area and another in the median. These are familiar structures. They appear to have developed as a direct result of the application of the AASHO Specifications (1).

The truss configuration was, at one time, almost a universal choice for all but very short-span highway bridges. It became recognized that this type of structure was not aesthetically pleasing. The modern welded girder and prestressed concrete long-span structures were developed to replace the truss. The resulting structures were more slender and presented a solid profile. Deflection and span-depth-ratio limitations continue in most present day highway bridge design specifications as an impediment to further improvement. These rules are rather arbitrary and, while they may have served suitably in the past, it is now recognized that relaxation is possible by means of more liberal regulations (2). Similar changes can be applied to overhead sign structures resulting in greater simplicity and improved appearance. An example of where this has been done is shown in Figure 2.

New highway safety practices (3) require the elimination of hazardous fixed objects from the roadside. Where this is impractical, adequate protective barriers are to be used. Overhead sign supports are not to be located in the gore area. Such structures are required to span the ramp exit pavement as well as the through lanes. Where flexible barriers are used, the location of overhead sign supports in narrow medians is undesirable, and spans clearing the roadways for both directions of traffic are necessary. Under these circumstances spans as long as 200 ft may be required to clear as many as 10 lanes of divided traffic and exit pavement, with adequate safe outside shoulder clearance, and capable of supporting up to four full-size freeway signs. The use of long-span monotubular sign structures as reported herein, allows these new highway safety practices to be met (Fig. 3).

A NEW DESIGN PHILOSOPHY

Beginning in 1967, a review of the AASHO Specifications (1) was carried out in conjunction with the design of several monotubular pipe frames for overhead spans. A detailed structural analysis of the behavior of a typical roadway lighting pole under specified loadings was also completed.

Figure 1. "Old style" overhead sign structure.

Figure 2. "New style" overhead sign structure (85-ft span; 14-in. pipe diameter).

The possibility of using large-diameter, thin-walled, single pipe sections in sign structures was enhanced in 1966 with the publication of the Second Edition of the Guide to Design Criteria for Metal Compression Members (4). The new Guide contained greatly increased slenderness ratios for local buckling of circular tubular members. The Revised Edition of AASHO (5) recognizes this information by including new limits on pipe radius/wall thickness, slenderness ratios. However, both the original and revised editions of AASHO require a limit on dead-load deflection of $d^2/400$ (in ft).

Figure 3. Long span provides clear gore area and flexibility of structure location (140-ft span; 20-in. pipe diameter).

It was found that adherence to this limit was not practical using reasonable pipe sizes. For example, if a typical sign panel has a vertical dimension of 10 ft (d = 10 ft), the limiting dead-load deflection would be $10^2/400 = 0.25$ ft, or 3 in. This applies irrespective of span length and requires that very deep and stiff structures be used, especially in long spans. The calculated dead-load deflections for the pipe-structure designs were found to increase with span length. Values exceeding 3 in. were calculated for all spans over 100 ft.

The AASHO deflection relationship $\Delta_{max} = d^2/400$ is obtained by equating the frequency of vortex shedding from a sign panel, $f_V = SV/d$, to the fundamental frequency of a simple span beam of uniformly distributed mass and stiffness, $f_O = \pi/2\sqrt{EIg/wl^4}$. The similarity of the expression for dead-load deflection at midspan, $\Delta_{max} = 5wl^4/384\ EI$, to the inverse of that under the radical sign, has led to substitution and evaluation, with a wind velocity of 80 mph, to obtain the AASHO relationship. The procedure implies that at a wind speed of 80 mph both the frequency of vortex shedding and the fundamental frequency of the structure are resonant. Evaluation of the two equations separately will show that this is most unlikely.

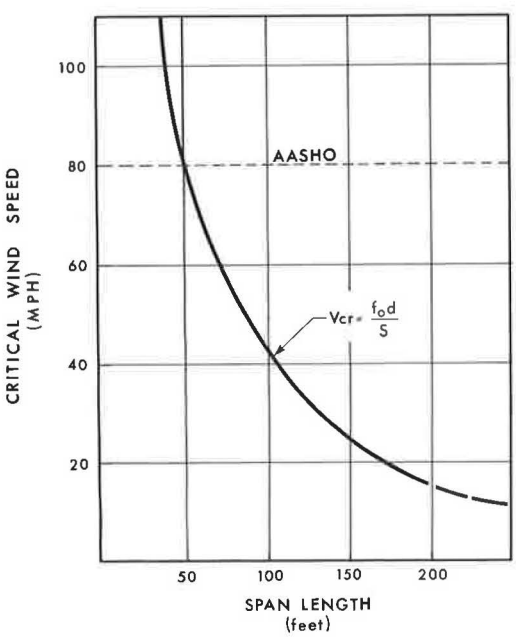

Figure 4. Critical wind-speed chart.

By substituting $f_O = f_V$, the so-called condition of resonance, and evaluating the equation for vortex shedding on each structure designed, a set of values of critical wind speed and span lengths was obtained. A curve representing these values is shown in Figure 4 which shows the critical wind speeds compared with the AASHO value of 80 mph. The suggestion is that the Specification grossly overestimates critical wind velocities for long-span sign structures.

In a similar manner, if the derived critical wind speeds for the condition of resonance are used for each span length, rather than 80 mph, a new set of deflection limits may be obtained. Figure 5 shows a curve representing these values and compares them to the AASHO limit of $d^2/400$. The observation made is that the Specification imposes too rigid a limitation on dead-load deflection for long-span sign structures.

The expression, $f_v = SV/d$, is also applicable to light poles if the diameter is used for the representative dimension d. The fundamental frequency of a cantilever beam of uniformly distributed mass and stiffness is given by $f_o = 7/4\pi\sqrt{EIg/wl^4}$. The equation for deflection at the free end of a cantilever beam under uniform transverse loading is $\Delta_{max} = wl^4/8EI$. Substitition of this, as has been done in the AASHO Specifications, leads to a limit of $\Delta_{max} = d^2/440$ (in ft), where d is the pole diameter in ft.

Evaluation of this expression for a typical steel light pole erected horizontally (representative diameter = 0.5 ft), results in a dead-load deflection of a $(0.5)^2/440 = 0.00056$ ft, or just 0.0068 in. The pole, not including the heavy luminaire, erected in a horizontal position would deflect several inches. Presumably, light poles as presently known would not have evolved had they been required to meet such a severe limitation. An analysis has indicated dead-load deflections at the tip of the mast arm for the standard 36-foot-high, 11-gage steel pole in the normal vertical position, with luminaire in place to be 3.06 in. vertical and 4.61 in. horizontal. Under design wind load the tip deflection normal to the plane of the pole was found to be 21.10 in. A recent research report (6) on similar light poles is of interest in that it shows that maximum dynamic-response effects may not be associated with design wind velocities, but rather with some value substantially less and perhaps less than half the design velocity.

On the basis of this investigation it was concluded that the AASHO limitation on deflection was not representative for design of long-span monotubular sign supports. It was also felt that a consistent philosophy should be reflected in the design of both light poles and sign supports. Similar, it not identical, materials are used. Foundations and methods of fixing structures to them may also be similar. The conditions of service and consequences of failure are quite alike. Neither structure is a particularly costly element in comparison to the total cost of the facility.

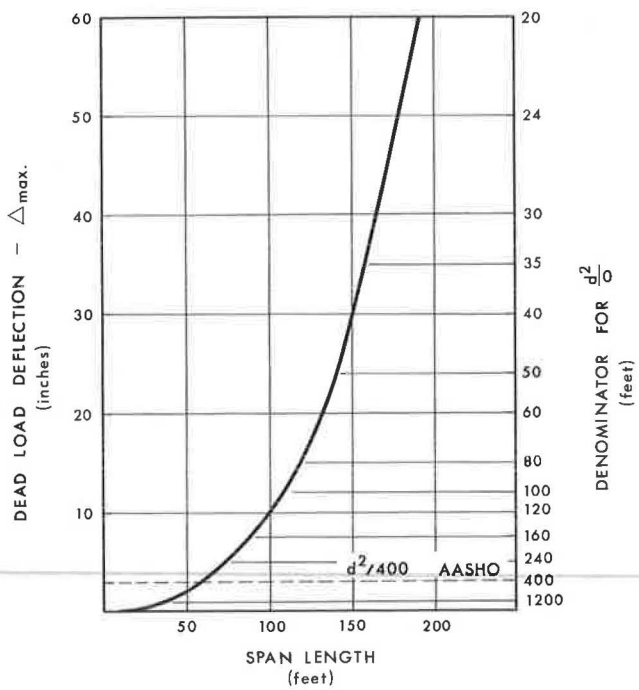

Figure 5. Deflection limitation chart.

APPLICATION AND OBSERVATION

The designs for several overhead pipe sign structures were completed in detail using AASHO group loadings and stress levels, and plans prepared for their construction. The spans varied in length from 85 to 200 ft. Frame analyses for loads and deflections were reviewed and found to be in excess of $d^2/400$, but very much less than the limits suggested in Figure 5. The calculated dead-load deflection at midspan was $7\frac{1}{2}$ in., and for a 200-ft span, $12\frac{1}{2}$ in. The calculated maximum horizontal deflection under design wind load (maximum gust speed 104 mph) for these structures is $24\frac{1}{2}$ in., $18\frac{1}{2}$ in., and $25\frac{1}{4}$., respectively. The 156-ft span is the longest built to date.

Details are shown on the accompanying Plan Sheets, Figures 6 and 7.

The effects of dynamic wind loading and structural damping on stress levels and deflections were not evaluated in the analysis. Essential to design that does not evaluate all stresses which may occur is the use of member and connection details leading to high-fatigue resistance. The pipe splices were detailed as flush butt, welds. High-strength, bolted field connections were located near the dead-load points of contraflexure. A

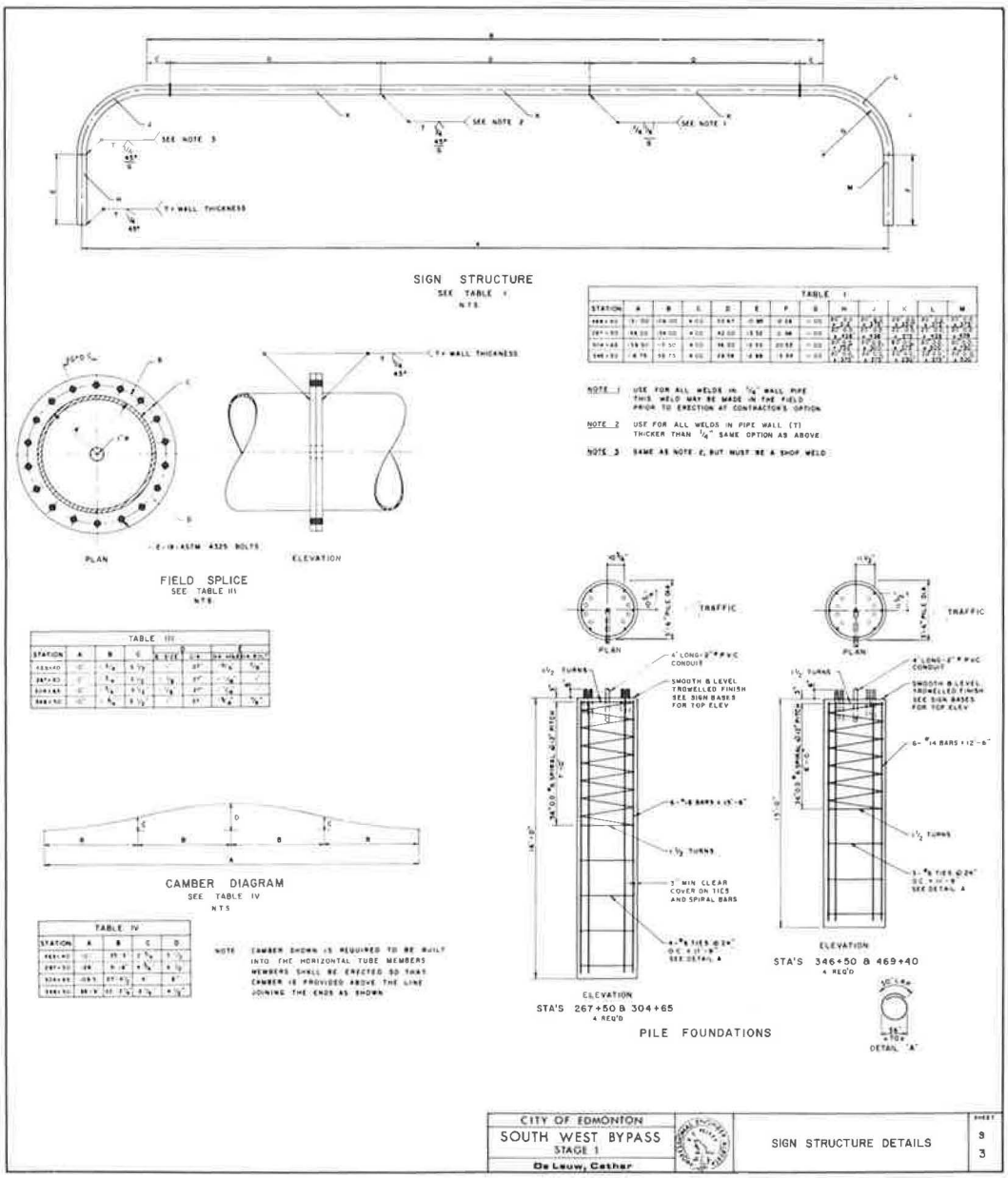

Figure 6.

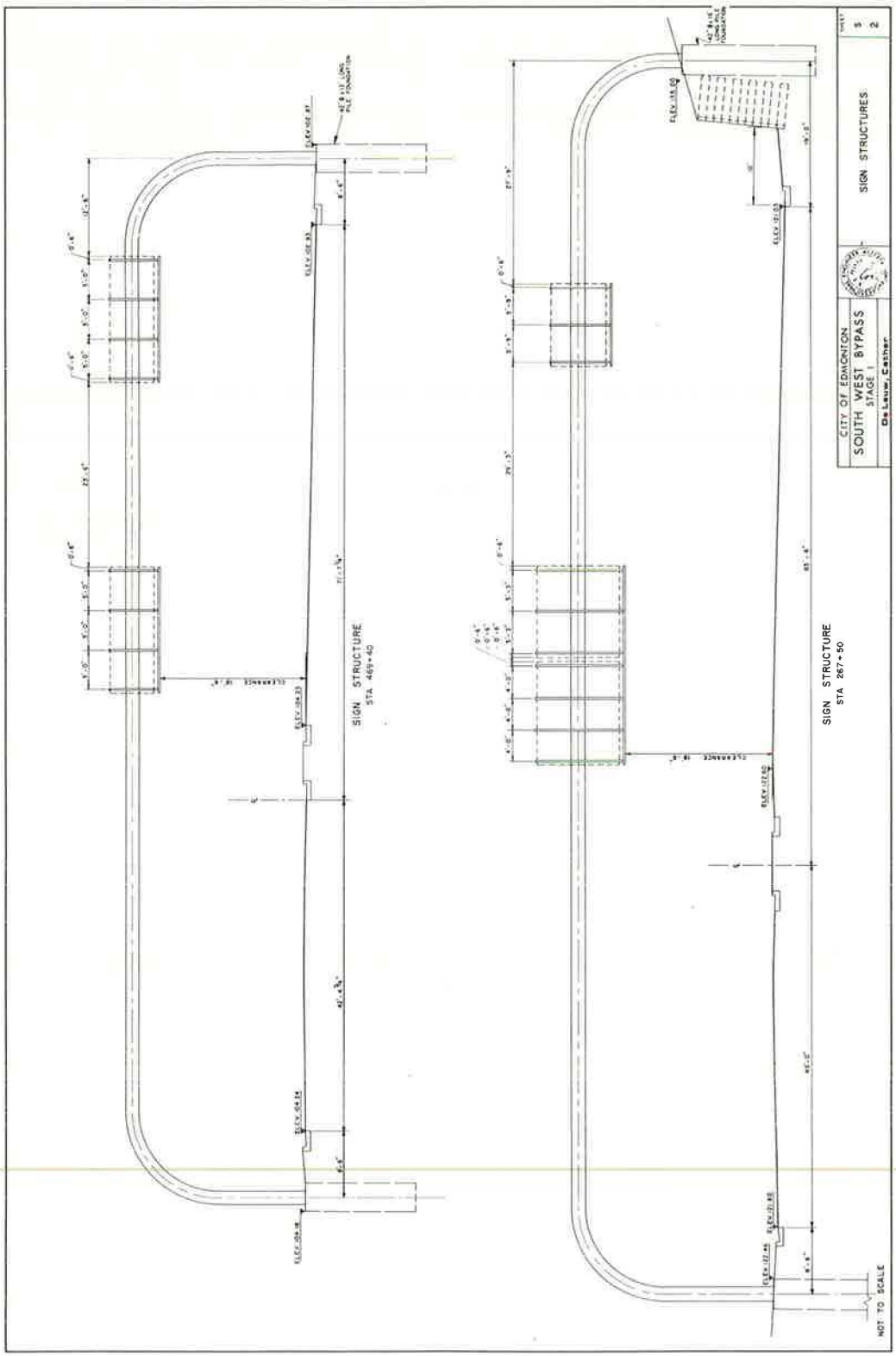
SIGN STRUCTURE
STA 469+40
SIGN STRUCTURE
STA 267+50
CITY OF EDMONTON
SOUTH WEST BYPASS
STAGE 1
SIGN STRUCTURES
NOT TO SCALE

Figure 7.

circular pipe section was selected for design because it was readily available and was similar in shape to the octagonal light poles used. A pipe was also a desirable section because, when used as a very slender flexural member, lateral-torsional buckling is not a problem. A pipe shape has a streamlined profile that results in lower wind-drag forces than for any other available section. The members are subject to high stresses due to loading in more than one plane. These stresses are effectively accommodated in the pipe section. The outside pipe diameter was uniform in any one structure. The pipe material conforms to ASTM Specification A53—Grade B. ASTM A36 material was used for all other shapes and plates.

The sign structures are supported by a single bored concrete pile beneath each vertical column. The AASHO Specifications (5) provide a chart intended for use in the design of embedded posts of this type. Unfortunately the loadings involved exceed the limits of the chart. A suitable method of design was found in the procedure suggested by Broms (7) for clay-type soils such as may occur at the site. A further paper by Broms provides a means for design in sandy and other cohesionless-type soils (8).

A structure combining sign panels over limited length and exposed main tubular member elsewhere, presents a highly complex system for vortex shedding and oscillation normal to the wind direction. Apparently on long circular cylindrical members a spanwise nonuniformity of vortex shedding also occurs over a wide range of Reynolds Numbers (9). It is likely that any mathematical analyses attempting to simulate actual behavior under these conditions would be suspect. More promising solutions are likely to be found in wind-tunnel tests using scale models and on field tests using full-scale structures.

Visual observations of all sign structures since installation have shown no unusual behavior. Vibrations have been nominal and noticeable only under close inspection. It is interesting to note that meteorological records, taken by the Canadian Department of Transport in the vicinity of the installations, show that since being erected in 1967 and 1968, wind-gust speeds in a direction approximately normal to the spans have reached a maximum value of a least 65 mph. Over the period of record available (nearly 30 years) the maximum recorded value of wind-gust speed is 82 mph. It is felt that this evidence establishes the acceptability of the aerodynamic performance of the structures.

Future development of long-span monotubular sign structures may benefit greatly from research presently being carried out under HRB sponsorship. Investigations are being continued on wind loads on louvered signs at the Texas Transportation Institute. An earlier report (10) has shown that wind-drag forces on nonsolid signs may be reduced 50 percent or more without impairing readability or target value. A significant recommendation is also made in favor of lower design wind speeds for highway sign loading. The continuation of this research, including testing of full-size installations, may show that a particular type and arrangement of louvers results in a "shroud effect" or "spoiler effect" preventing the formation and shedding of vortices as well as substantially reducing wind forces on sign panels. The results will be anticipated with enthusiasm since the AASHO Group 2 loading, combining dead-load and wind-load effects, governs the design of long-span sign structures.

Equally important research is being directed toward the adaptation of breakaway behavior to large supporting members of long-span overhead sign structures (11). Such members will presumably be adaptable to all overhead monotubular spans supported on three or more columns. In instances where support columns are insufficiently offset from the edge of pavement, their use will eliminate the need for protective barriers and the hazard they represent.

FABRICATION, ERECTION, AND COSTS

The sign-support structures were shop welded by manual procedures. All main pipe welds were full-penetration butt welds. Low-hydrogen electrodes of Class E7018 were specified for this purpose. Visual inspection of the joints were made after fit-up was complete, during the welding operation, and upon completion. No other form of weld inspection was performed. Some weld splices were made on site in order to reduce shipping lengths of members.

The 90-deg bends were manufactured by heat curving originally straight lengths of pipe. Experience with these bends has shown that wall thicknesses obtained from structural design may not be adequate for fabrication. For each pipe diameter and wall thickness there is a minimum radius of bend which can be successfully made. Smaller radii result in the development of buckles in the pipe wall on the inside of the bend. To avoid this condition the design thickness and radius of bend should be reviewed and an acceptable combination chosen to satisfy the relationship $t_{min} = 2.5\ d/R$.

Figure 8. Simple three-piece erection—fast bolting-up operation (120-ft span; 20-in. pipe diameter).

Erection of the sign supports was easily and quickly carried out. As shown in Figure 8, vertical members including the 90-deg bends were first erected on the foundation piles. The anchor bolts had previously been accurately located in concrete piles by means of precise surveys. The horizontal member was then hoisted into position and the bolted splice made. ASTM A325 high-strength bolts in $^{7}/_{8}$-in.-and 1-in.-diameter size were used. Field tightening was by the turn-of-the-nut method producing the required tension in the bolts. The entire erection operation for each sign structure was accomplished in less than one hour.

Painting for both shop and field coats was a simple operation because of the clean and continuous surface of the pipe. Internal surfaces were left unpainted except for those within reach of a handhole at the base of each leg. A 1-in.-radius hole in the splice plates provides for the electrical wiring to pass through the verticals and bend into the horizontal members. A small hole, field cut in the bottom of the horizontal member, leads the wiring to the luminaires. The concept of using an unpainted interior is similar to that employed with light poles and is felt to be quite acceptable for this type of structure. Experience with light poles has shown that metal oxidation is a problem only in the region of the base-to-pole connection. This part of the sign support is open to inspection and repainting if necessary.

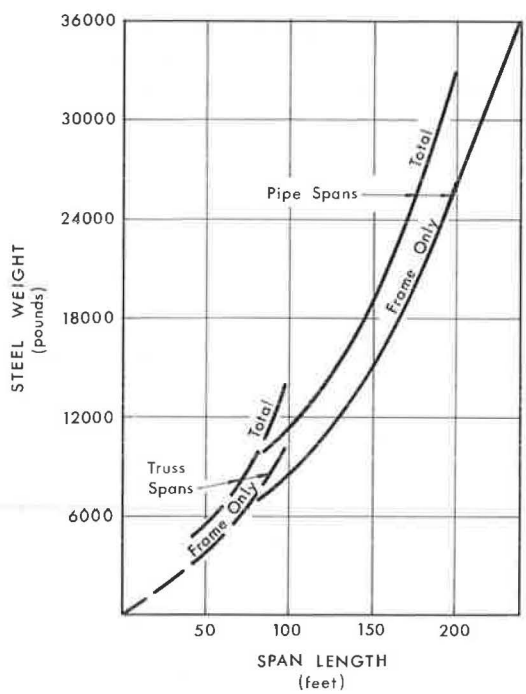

Figure 9. Steel weight chart.

The chart of steel weight plotted against span length shown in Figure 9 compares the pipe support structures to available information on truss span sign supports of similar design and details. The curves indicate that the weight of steel required in pipe supports is not excessive when compared to truss spans. Some advantages in terms of weight may be indicated in spans over 100 ft in length.

Included in the weight curves shown are the panel stiffeners and luminaire supports. In all cases these members were designed to support a temporary walkway and live-load forces as called for in the AASHO Specifications. A permanent walkway has not been installed as the intention is to carry out routine maintenance from a basket arm or snorkle truck operated from the

shoulder area. For the infrequent occasions when more extended work or reaches exceeding the boom length of the truck are required, a portable walkway and light tubular railing will be clamped into place on the permanent supports to provide a safe work platform.

The construction of the sign support structures was carried out under contract. The contract included the construction of foundations, the supply, erection, and both shop and field painting of the steel frames, panel stiffeners and luminaire supports. The total contract price for the 85-ft-span pipe structures built during 1967 was $6,170.00 per span. The 1968 contract price of the four longer pipe span structures was $46,643.00 in total. Not included in the contract were items of supply and installation of sign panels, luminaires, and wiring.

CONCLUSIONS

The results of this study and the subsequent full-scale construction have shown the use of closed-section, single-member frames for long-span sign structures to be both economical and attractive. The service performance during the two and three years since installation has been excellent. The design of these frames would not be possible if the specified dead-load deflection limitation in AASHO had been met. Reliable new limitations have not been defined, but it has been demonstrated that existing limitations can be greatly relaxed.

The behavior of highway-sign support structures under dynamic wind loading appears highly complex, especially at the very high Reynolds Numbers involved. Further progress in evaluating the oscillating forces accompanying such loading and their effects on the support structures may be facilitated by wind tunnel model studies and field research on full-scale installations. In the meantime, monotubular frames of characteristics similar to those shown here may be used to achieve simplicity and safety in aesthetically pleasing structures for spans as long as 200 ft.

ACKNOWLEDGMENT

As a part of this study, use is made of information taken from several designs completed for the City of Edmonton, Alberta, by De Leuw, Cather and Company of Canada Limited. The author wishes to thank Mr. William E. Gillespie, Roadway Design Engineer, City of Edmonton, for permission to include this material.

The author also wishes to express his appreciation to Mr. Jack E. Leisch, Vice-President, De Leuw, Cather and Company of Canada Limited, and President of Jack E. Leisch and Associates, Evanston, Illinois, for helpful suggestions and encouragement during the preparation of this report.

REFERENCES

1. Specifications for the Design and Construction of Structural Supports for Highway Signs. American Association of State Highway Officials, 1961.
2. Committee on Dynamics and Field Testing of Bridges. Highway Research Board, Highway Research Circular, No. 107, February 1970.
3. Handbook of Highway Safety Design and Operating Practices. U.S. Department of Transportation, Federal Highway Administration, May 1968 and Supplements.
4. Guide to Design Criteria for Metal Compression Members, Second Edition. Column Research Council. 1966.
5. Revised Edition of Reference (1), dated 1968.
6. Ross, H. E., and Edwards, T. C. Wind Induced Vibrations in Light Poles. Proceedings of American Society of Civil Engineers, Journal of Structural Division, Paper No. 7383, June 1970.
7. Broms, B. B. Lateral Resistance of Piles in Cohesive Soils. Proceedings ASCE, Journal of Soils Mechanics and Foundation Engineering Division, Paper No. 3825, March 1964.
8. Broms, B. B. Lateral Resistance of Piles in Cohesionless Soils. Proceedings ASCE, Journal of Soils Mechanics and Foundation Engineering Division, Paper No. 3909, May 1964.

9. Leinhard, J. H. Synopsis of Lift, Drag and Vortex Frequency Data for Rigid Circular Cylinders. Bulletin 300, Washington State University, 1966.
10. Highway Sign Support Structures, Volume 2, Wind Loads on Roadside Signs. Texas Transportation Institute, Texas A&M University, July 1967.
11. Taminini, F. J. Designing "Fail-Safe" Structures for Highway Safety. Bureau of Public Roads, Washington, D. C., April 1970.

Appendix

SYMBOLS USED IN THIS PAPER

d = outside diameter of pole or pipe (feet), also sign panel height (feet);
E = modulus of elasticity (pounds/inch^2);
f_0 = fundamental frequency of vibrating system (cycles/second);
f_V = vortex shedding frequency (cycles/second);
g = acceleration due to gravity (386.4 inches/second);
I = moment of inertia (inches^4);
l = span length (inches);
R = centerline radius of pipe bend (feet);
S = Strouhal number (usually 0.2);
t_{min} = minimum wall thickness of pipe (inches);
V = wind velocity (feet/second);
w = weight of vibrating system per unit length (pounds/inch); and
Δ_{max} = maximum static (dead-load) deflection (inches).

BUCKLING STRESS FORMULAS FOR OVERHEAD SIGN BRIDGE SUPPORTS

R. H. Gunderson, A. Cetiner, and R. M. Olson, Texas A&M University

Contemporary freeway operations require large signs over traffic lanes. These signs are usually attached to trusses mounted on vertical supports. The supports are essentially restrained cantilever beams. The 1968 AASHO Specifications (1) require, among other things, that the critical buckling stress be limited by a formula based on theoretical and experimental investigations of a simple beam subjected to loads which produce pure bending (8, 9, 10). The purpose of this study is to examine this formula to determine its applicability to highway sign supports, and to develop a suitable alternate requirement. Rigorous adherence to the present AASHO requirement results in uneconomical open sections for overhead sign bridge supports which are fixed at the base, restrained from lateral movement at the top, and are subjected to wind and dead loads which produce lateral, transverse, axial, and moment forces. The same conditions exist on roadside signs with two or more supports, but the critical buckling stress requirement does not greatly affect the selection of economical flanged shapes for such supports. A formula is developed for critical buckling stress, and it is shown that this formula is in agreement with available test results. Comparisons of other theoretical buckling formulas with test data are also presented.

•THIS paper examines the critical buckling stress requirements for the design of supports for overhead sign bridges. The discussion which follows is intended to show that current AASHO Specification (1) requirement Section 6(a)(3) for critical buckling stress is uneconomical, because its application leads to heavier sections than are needed. It will be shown that compliance with the critical buckling stress requirement is not necessary, because it is based on theoretical and experimental investigations of a beam subjected to pure bending, whereas an overhead sign bridge support is a cantilever beam column in which the axial forces are small compared to other design loads. Economical design is always desirable, but, in addition, safety of the traveling public is also a prime consideration of contemporary design; and to meet the latter consideration, it becomes imperative to use the lightest supports required to meet stress requirements, maintain structural stability, and meet the other criteria of sound design procedure. Symbols and nomenclature used in this paper are shown in the appendix.

The AASHO Specifications for the Design and Construction of Structural Supports for Highway Signs (1), cites Formula 20 of the Design Manual for High Strength Steels (2) as its criterion for buckling stresses. This formula is:

$$f_{cr} = \frac{\pi^2 E}{2\left(\frac{L}{d}\right)^2}\sqrt{\left(\frac{I_y}{2I_x}\right)^2 + \frac{KI_y}{2(1+\mu)\,I_x^2}\left(\frac{L}{\pi d}\right)^2} \qquad (1)$$

Sponsored by Committee on Traffic Safety Barriers and Sign, Signal and Lighting Supports and presented at the 50th Annual Meeting.

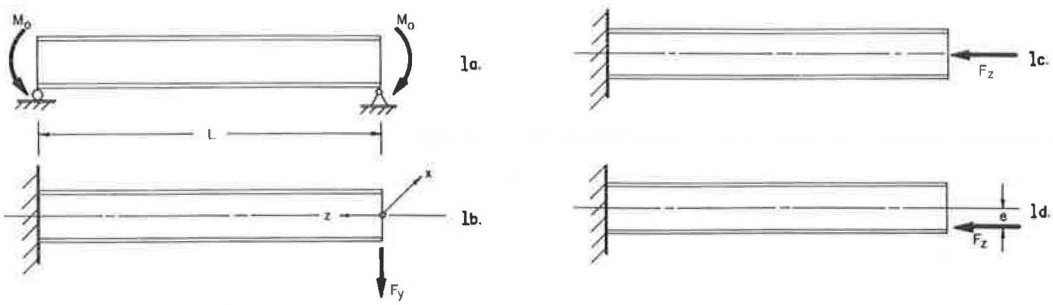

Figure 1. Support conditions and loadings for theoretical buckling cases.

This formula was derived and investigated experimentally by Winter (8, 10); deVries (9) showed that when I_x is several times I_y, this relation reduces to:

$$f_{cr} = \frac{18.83 \times 10^6}{\frac{Ld}{bt}} \tag{2}$$

which is presented as Formula 21 in the U.S.S. Design Manual (2). Formulas 20 and 21 apply to lateral buckling of beams in pure bending (Fig. 1a). Timoshenko (5) gives a formula similar to Formula 20, and also presents an equation for lateral buckling of a cantilever beam under transverse end load (Fig. 1b), which will be discussed later, as Eq. 5.

The theoretical buckling stress for a perfectly straight slender member under axial compression (Fig. 1c) is given by the well known Euler equation

$$f_{cr} = \frac{\Pi^2 E}{\left(\frac{K_y L}{r_y}\right)^2} \tag{3}$$

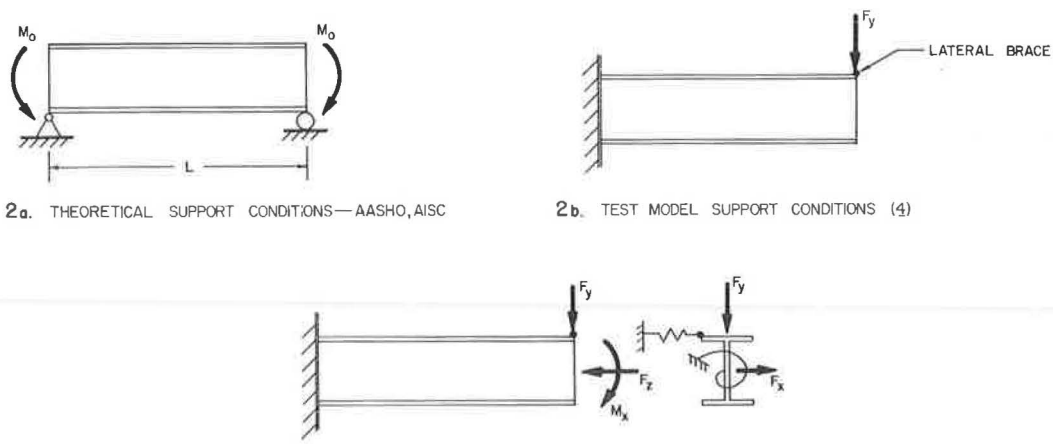

2a. THEORETICAL SUPPORT CONDITIONS—AASHO, AISC

2b. TEST MODEL SUPPORT CONDITIONS (4)

2c. OVERHEAD SIGN BRIDGE SUPPORT CONDITIONS

Figure 2. Support conditions and loadings.

Another expression for determining critical axial stress on columns with a small amount of eccentricity (Fig. 1d) is the Secant Formula

$$f_{cr} = \frac{P}{A}\left[1 + \frac{ec}{r^2}\sec\left(\frac{L}{2r}\sqrt{\frac{P}{AE}}\right)\right] \tag{4}$$

All of these expressions for critical buckling stress relate the geometrical properties of a member and its modulus of elasticity. The elastic modulus for steel is constant for all grades, but the yield strengths vary widely. Lighter members fabricated from higher strength steels are more susceptible to buckling than members fabricated from lower strength steels. Thus, the critical buckling stress governs more often as the strength of the steel increases. An overhead sign bridge support is subjected to a combination of loads (Fig. 2c). However, no formulas for calculating critical stress exist for general loading (6).

CANTILEVER BEAM COLUMNS WITH END RESTRAINT

Timoshenko (5) gives the following formula for critical buckling load of a cantilever beam under transverse end load (Fig. 1b).

$$P_{cr} = \frac{4.013\sqrt{EI_yGK}}{\left(1 - \sqrt{\frac{EI_yd^2}{4GKL^2}}\right)^2 L^2}\left(1 - \frac{a}{L}\sqrt{\frac{EI_y}{GK}}\right) \tag{5}$$

The term $\left(1 - \frac{a}{L}\sqrt{\frac{EI_y}{GK}}\right)$ is a correction factor to account for the load being applied at points other than the centroid. If the load is applied to the upper flange, a is $\frac{d}{2}$. The maximum bending stress would occur at the fixed end:

$$F_{cr} = \frac{Mc}{I} = \frac{P_{cr}\cdot L\cdot\frac{d}{2}}{I_x} = \frac{4.013}{I_x}\left(\frac{d}{2L}\right)\frac{\sqrt{EI_yGK}}{\left(1 - \frac{d}{2L}\sqrt{\frac{EI_y}{GK}}\right)} \tag{6}$$

If the effective lengths are taken into account, the formula becomes:

$$F_{cr} = 4.013\left(\frac{d}{2L}\right)\left(\frac{K_x^2}{I_x}\right)\frac{\sqrt{EG}\sqrt{\frac{I_y}{K_y^2}\cdot\frac{K}{K_z^2}}}{\left(1 - \frac{d}{2L}\sqrt{\frac{E}{G}\frac{I_y}{K_y^2}\cdot\frac{K_z^2}{K}}\right)} \tag{7}$$

where K_x, K_y, and K_z were each 2.0 in the original derivation for a cantilever beam.

This expression clearly shows that this type of buckling is a combination of weak axis bending and torsion. The effective length factor, K_z, refers to the effective length of the compression flange during buckling and is therefore the same as K_y, and thus, K_z will be replaced by K_y. Equation 7 can be written as

$$F_{cr} = 4.013 \left(\frac{d}{2L}\right)\left(\frac{K_x^2}{I_x K_y^2}\right) \frac{\sqrt{EGI_y K}}{\left(1 - \frac{d}{2L}\sqrt{\frac{E}{G}\frac{I_y}{K}}\right)} \tag{8}$$

The effective length, $K_y L$, can be obtained from Figure C1.8.3 of the AISC Manual of Steel Construction (3) using a G_A (flexibility coefficient) for the partially restrained end obtained in the following manner (Fig. 3).

The point "A" denotes the point of lateral support.

$$\delta_P = \frac{PL^3}{3E\left(\frac{I_y}{2}\right)} \tag{9}$$

$$\delta_T = \theta\left(\frac{d}{2} + e\right) = \frac{TL}{GK}\left(\frac{d}{2} + e\right) = \frac{PL\left(\frac{d}{2} + e\right)^2}{GK} \tag{10}$$

where δ_P is the lateral displacement of the compression flange due to a fictitious lateral load, P, and δ_T is the lateral displacement resulting in a resisting torque, T.

$$G_A = \frac{\delta_T}{\delta_P} = \frac{3}{2}\frac{EI_y}{GK}\left(\frac{d}{L}\right)^2\left(\frac{1}{2} + \frac{e}{d}\right)^2 \tag{11}$$

The deviation between test results and theoretical calculations increase as the members become lighter. It seems logical, therefore, to incorporate the term I_x/I_y into the factor of safety to be applied to the theoretical stress. Assume a factor of safety in the form,

$$F.S. = 2\left[1 + \left(\frac{1}{100}\frac{I_x}{I_y}\right)^2\right] \tag{12}$$

This factor of safety when applied to the theoretical stress is always greater than 2.0 and, when applied to the test results, the real margin of safety ranges from 1.67 for low ratios of I_x/I_y to 2.0 for very high values of I_x/I_y. The factor of safety is approximately 2.0 for most sections which are used for sign supports.

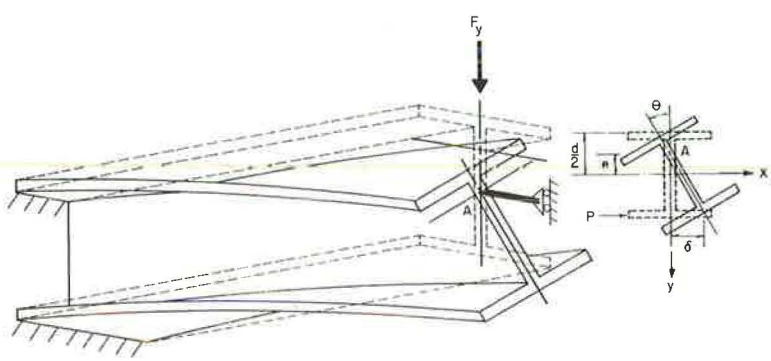

Figure 3. Model support conditions.

TAPERED BEAM COLUMNS

When the load on a cantilever beam is limited by yielding at the fixed end, it is apparent that some saving in material (and thus a saving in weight) can be made by tapering the web depth and flange width. A series of load tests were conducted by Krefeld (4) on cantilever beams with partial end restraint, subjected to end-point loads. A lateral end brace was attached to the tension flange which allowed rotation of the end, but did not permit the tension flange to move laterally (Fig. 2b), and the lateral brace restricted the motion of the compression flange also. These test conditions more closely approximate the loading and end conditions for an overhead sign bridge than those in any of the theoretical derivations; and, as shown in Figures 4 and 5, the experimental failure stresses are much larger than predicted by the formulas listed in Table 1.

Krefeld's test results led to the following empirical equations for untapered beams with end load and end brace:

$$f_{cr} = \frac{80{,}000{,}000}{\frac{Ld}{bt}} \text{ psi} \qquad \text{for } 5{,}000 > \frac{Ld}{bt} > 2{,}500 \tag{13}$$

and

$$f_{cr} = \frac{110{,}000{,}000}{\frac{Ld}{bt}} - 7{,}000 \text{ psi} \qquad \text{for } 5{,}000 > \frac{Ld}{bt} > 1{,}000 \tag{14}$$

where f_{cr} is the nominal stress at the support when elastic buckling occurs. Equation 13, although simpler, becomes increasingly conservative for high-yield-point materials below the limits of Ld/bt specified.

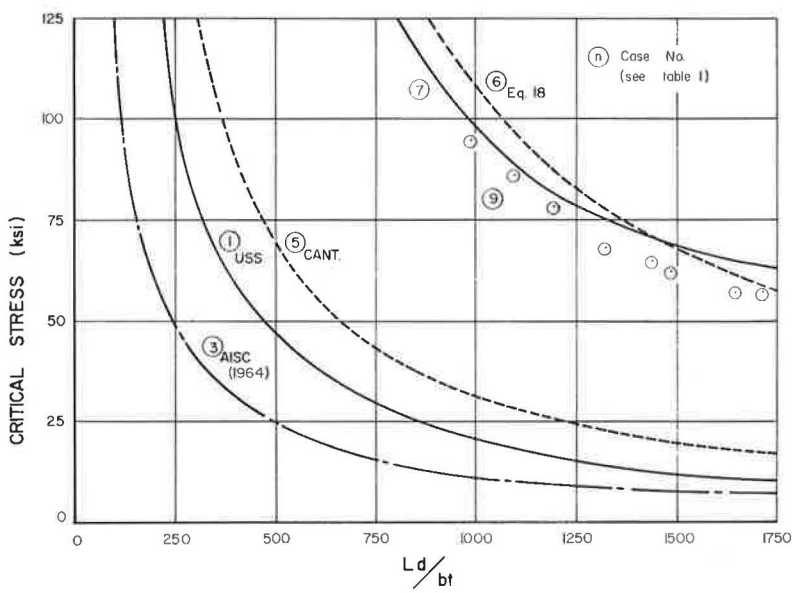

Figure 4. Comparison of critical stresses versus Ld/bt from various theoretical formulas and test results.

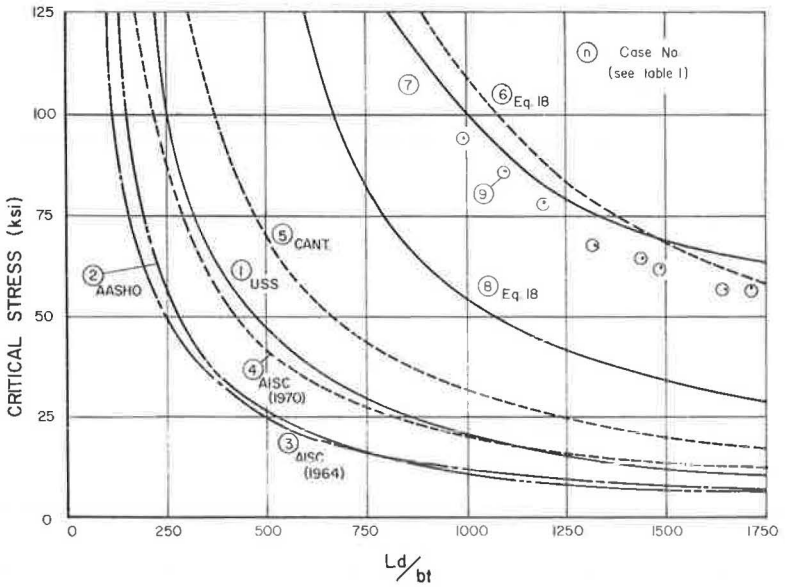

Figure 5. Comparison of critical stresses versus Ld/bt from various theoretical formulas with safety factors and test results.

Krefeld (4) noted

> . . . that the flange stress at points within the span increases with increasing taper and that for extreme tapers the flange stress may be greater at points near the end of the cantilever than at the support.

He introduced a stress-reduction factor for tapered beams, R, which is defined as

> . . . the ratio of the nominal stress at the support of a wedge beam to that of an untapered beam having the same section at the support when elastic buckling occurred.

TABLE 1

CRITICAL STRESS CASES

Case	Description	Source
1	Lateral buckling of simple beam in pure bending	USS Design Manual (2) Formula 20 (see also References 8, 9, and 10)
2	USS Formula 20 with a 1.8 safety factor	AASHO Specifications (1)
3	Allowable stress formula based on lateral buckling	AISC Steel Manual (3), Sixth Edition, 1964
4	Allowable stress formula based on lateral buckling modified to include effects of end moments	AISC Steel Manual (12), Seventh Edition, 1970
5	Lateral buckling of cantilever beams under transverse end load	Timoshenko (5), p. 258
6	Lateral buckling of restrained cantilever—includes effects of end conditions	Proposed Stress Formula, Equation 18
7	Lateral buckling of restrained cantilever—modified Equation 18	Equation 20
8	Proposed critical stress formula with 2.0 safety factor	Equation 18
9	Test data	Krefeld et al. (4)

The reduction factor is a function of the section moduli and flange dimensions at each end of the beam

$$R = F\left[\left(\frac{Z_0}{Z_1}\right), \left(\frac{b_0 d_1}{b_1 d_0}\right)\right] \tag{15}$$

The critical stress producing buckling of a tapered beam with a given span was found to vary with the parameter

$$\alpha = \frac{Z_0}{Z_1}\left(\frac{b_0 d_1}{b_1 d_0}\right)^{3/2} \tag{16}$$

and this equation agrees with test results. The reduction factor can be expressed in terms of α as follows; for end load, with end brace:

$$R = \frac{7 + \alpha}{5 + 3\alpha} \tag{17}$$

From this formula, it is possible to determine maximum tapers such that no reduction is necessary. Note that when R = 1.0, α = 1.0. Therefore, no reduction is necessary when α is 1.0. If there is an axial load in addition to the lateral load, then the taper must be less than that calculated by the above formula. A reasonable upper limit appears to be $Z_0/Z_1 = 4.0$.

PROPOSED CRITICAL STRESS FORMULA

The critical stress formula (Eq. 8) can now be rewritten to include the effects of taper on the column. The effects of eccentricities of loading, residual stresses, and imperfections are considered to be adequately compensated for in the factor of safety.

The proposed critical stress formula to be used for overhead sign bridge supports is

$$F_{cr} = \frac{1}{F.S.}\,\frac{R}{I_x}\left(\frac{2d}{L}\right)\left(\frac{K_x}{K_y}\right)^2 \frac{\sqrt{EI_y GK}}{\left(1 - \frac{d}{2L}\sqrt{\frac{EI_y}{GK}}\right)} \tag{18}$$

The terms in this equation are defined as:

- F.S. = factor of safety (Eq. 12);
- d/L = depth/length;
- K_x = effective length factor based on end conditions for bending about the x-axis;
- K_y = effective length factor based on end conditions for bending of the compression flange about the y-axis. This involves a special flexibility coefficent, G_A, to account for possible twisting of top of column (Eq. 11). After the G values are known, the K values are obtained from Figure C1.8.3 of the AISC Manual of Steel Construction (3);
- E, G = modulus of elasticity, shearing modulus;
- K = torsional rigidity of section, for I and wide flange sections (Eq. 19); and
- R = a parameter to account for taper (Eq. 17).

If the web of the member contributes very little to I_x, I_y, and K, the following approximate expressions can be used (10).

$$I_x \doteq 2\,bt_f\left(\frac{d}{2}\right)^2, \quad I_y \doteq \frac{2t_f b^3}{12}, \quad K \doteq \frac{2}{3}\,bt_f^3 \tag{19}$$

Substitution of these terms into Eq. 18 yields:

$$F_{cr} \doteq \frac{4R}{3(F.S.)}\left(\frac{K_x}{K_y}\right)^2 \frac{\sqrt{EG}}{\left(\frac{Ld}{bt}\right)} \left[\frac{1}{1 - \frac{1}{4}\frac{\left(\frac{d}{t}\right)^2}{\left(\frac{Ld}{bt}\right)}\sqrt{\frac{E}{G}}}\right] \tag{20}$$

This equation yields allowable stress values which are usually a few percent higher than Eq. 18. This is comparable to Formula 5 of the AISC Code (3) derived by deVries (9). It incorporates a factor to correct for the position of the load since the load is usually applied to the flanges (Eq. 5). The last term in the denominator could be set equal to unity since Ld/bt is usually quite large. If typical values of the material constants for steel are substituted into the above equation ($E = 30 \times 10^6$ psi, $G = 11.5 \times 10^6$ psi),

$$F_{cr} \doteq \frac{24{,}800{,}000}{\left(\frac{Ld}{bt}\right)}\left(\frac{K_x}{K_y}\right)^2 \frac{R}{F.S.} \left[\frac{1}{1 - 0.4\frac{\left(\frac{d}{t}\right)^2}{\left(\frac{Ld}{bt}\right)}}\right] \tag{21}$$

A conservative approximation for the critical stress for the case of a restrained cantilever, as shown in Figure 2b, can be obtained by using the following values:

$$\begin{aligned} K_x &= 2.0 \\ K_y &\doteq 1.0 \\ R &= 1.0 \end{aligned} \qquad \left[1 - 0.4\frac{\left(\frac{d}{t}\right)^2}{\left(\frac{Ld}{bt}\right)}\right] \doteq 1.0 \tag{22}$$

Equation 21 now reduces to

$$F_{cr} = \frac{99{,}000{,}000}{\frac{Ld}{bt}\,(F.S.)}\ \text{psi} \tag{23}$$

This compares very closely with Krefeld's empirical critical stress formula for this case given in Eq. 14. This is similar in form to the critical stress formulas for simple beams subjected to end moments derived by deVries (9) and Winter (10) (i.e., the present AASHO formula).

This critical stress determined by Eq. 18 or 20 would be compared with the allowable bending stress, F_b. Equation 23 could be used for the specific case of the overhead sign bridge support. The lesser of the two values would be used for F_b in the AASHO interaction formula.

$$\frac{f_a}{F_a} + \frac{f_b}{F_b} + \left(\frac{f_v}{F_v}\right)^2 \leq 1.0 \tag{24}$$

The effects of lateral loading would be taken into account by using

$$\frac{f_a}{F_a} + \frac{f_{bx}}{F_{bx}} + \frac{f_{by}}{F_{by}} + \left(\frac{f_{vx}}{F_{vx}}\right)^2 + \left(\frac{f_{vy}}{F_{vy}}\right)^2 \leq 1.0 \qquad (25)$$

COMPARISON OF CRITICAL STRESS FORMULAS

The graphs (Figs. 4 and 5) show various critical stress formulas, as described in Table 1. In each case, it is assumed that the stresses are below the yield point. The Krefeld test results (4) are for relatively light sections with high ratios of I_x/I_y. The tests were performed on tapered and untapered cantilever beams with lateral restraint of the tension flange at the point of application of the transverse load (Fig. 2b). This closely approximates the conditions existing on an overhead sign bridge support. More detailed graphs are given in a Texas Transportation Institute Technical Memorandum (11).

The proposed critical buckling stress formula, Eq. 18, closely predicts the buckling stresses determined by the tests because it has the ability to account for different end conditions through the effective-length factors K_x and K_y.

The 1970 AISC Specifications (12) modify the 1964 AISC allowable bending stress equations (3) to account for end moments and, in general, are less conservative (by a factor of 1 to 2.3). For the case of a restrained cantilever beam with no moment at the free end, the curve in Case 3 is shifted upward by a factor of 1.75 (Case 4).

Figure 4 has no safety factors applied to the U. S. S. Manual (2) formulas or the present formula. The AISC (3) formula has a built in factor of 1.67 or greater. Figure 5 applies safety factors to the curves in Figure 4. The AASHO Specifications (1) require a safety factor of 1.8 applied to the U. S. S. formula and closely matches the AISC (3) formula. A safety factor of 2.0 is applied to the proposed critical stress formula (Eq. 18).

With the factors of safety applied, the buckling stress predicted by the proposed formula is approximately 4.8 times the stress determined by the current AASHO Specifications. If a safety factor of 3.0 is applied to the proposed critical stress formula, the predicted stress would be 3.2 times the AASHO Specifications. If buckling stress is the limiting factor in the design, the use of the proposed formula could result in significant savings in material.

The proposed formula appears to be sufficiently conservative for overhead sign bridge supports and the AASHO requirement seems to be too conservative. This is of significant importance in the design of breakaway supports in which the mass of the support must be kept to a minimum in order to limit damage to vehicles and to prevent injury to passengers.

DISCUSSION

The AASHO Specifications specify two wind-load combinations: (a) full normal load (F_y) plus a 0.2 lateral component (F_x); and (b) a 0.6 normal load plus a 0.3 lateral component. The lateral component causes a lateral displacement of the top of the support and, of course, results in a lateral bending stress. Since this bending is taking place about the weak axis, this can have a significant contribution to the interaction formula.

There has been some discussion as to the effect of this lateral load on the critical stress formula. It definitely will have some effect. However, inclusion of this lateral force results in a nonlinear, large deflection problem, not an eigen-value buckling problem, and it thus cannot be incorporated into the critical stress formula. The critical stress formula was based on support conditions and loadings, as shown in Figure 2b. An actual sign bridge support is connected to the truss or to the sign at more than one point. Thus, it has more than one lateral support point. The support conditions at the upper end are as follows:

1. Unrestrained against normal translation (y-direction).
2. Unrestrained against rotation about the major axis (x-axis).
3. Elastically restrained against rotation about the minor axis (may be considered rigidly restrained in most cases due to the stiffness of the truss).

4. Elastically restrained against lateral translation.
5. Elastically restrained against torsional rotation (may be considered rigidly restrained if firmly fastened to truss).

The only exception to these conditions is a roadside sign with a single support, in which case there is no lateral or rotational support and both K_x and K_y are 2.0 (7).

The critical stress formula is based on these support conditions at the upper end:

1. Unrestrained against normal translation (y-direction).
2. Unrestrained against rotation about the major axis (x-axis).
3. Unrestrained against rotation about the minor axis.
4. Restrained against lateral translation of tension flange only.
5. Elastically restrained against torsional rotation due to the lateral brace.

By comparing the end conditions for overhead sign bridge supports and the model on which the critical stress formula is based, it is apparent that the model restraints are much less rigid than that provided by field conditions. Therefore, it appears that the formula, when applied to actual cases, will have a factor of safety larger than 2.0 in spite of the fact that the lateral load has some effect on decreasing the critical stress.

The lateral displacement will have some effect on the actual critical stress. However, the lateral displacement is restrained by the framework between the supports. It is the authors' considered opinion that the effects of lateral displacement are adequately accounted for in the interaction formula.

The effect which the lateral load has on the critical stress can be determined from a nonlinear computer program; such a procedure is discussed briefly in a Texas Transportation Institute Technical Memorandum (11). Use of this nonlinear program in conjunction with full-scale tests would form the basis for important theoretical work in this area.

CONCLUSIONS AND RECOMMENDATIONS

This report considers critical buckling stresses in open sections. The major conclusion is that the present AASHO critical buckling stress formula is overly conservative when applied to sign supports. A critical stress formula was developed for restrained cantilevers which closely approximates the boundary conditions existing on an overhead sign bridge. The buckling stress criterion may not govern for lower strength steels. However, it may be the limiting stress for higher strength steels which are being used increasingly to reduce the support mass.

The critical stress formula proposed in this report is recommended for consideration for adoption into future AASHO Specifications. Areas which might be explored in more detail include: (a) full-scale tests on large wide flange shapes to determine critical stresses under various loadings and end restraints [an extension of the Krefeld study (4)]; (b) development of a finite-element buckling program to include effects of lateral-torsional buckling; (c) correlation of proposed critical stress formula (Eq. 18) with (a) and (b) above; and (d) determination of the validity of the use of an interaction formula of the form of Eq. 25.

It is apparent that application of the AASHO Specifications (1) results in a grossly overdesigned, double-tapered column as tested by Krefeld (4), and as shown in Figures 4 and 5.

The buckling problem is dependent on the conditions of end restraint. Thus, requirements for critical stress should provide means for accounting for various end conditions. The proposed formula has this flexibility.

ACKNOWLEDGMENT

This study was sponsored at the Texas Transportation Institute as part of a multi-states' cooperative research endeavor financed under the Highway Planning and Research Program by a contract with the Federal Highway Administration, Department of Transportation. The research was made possible through the cooperative highway department participation of: Alabama, Arkansas, Connecticut, Florida, Georgia,

Hawaii, Kentucky, Louisiana, Maryland, Michigan, Mississippi, Montana, Nebraska, New Hampshire, New Mexico, Rhode Island, South Dakota, Tennessee, Texas, West Virginia, Wyoming, and the District of Columbia. The opinions, findings, and conclusions expressed in this paper are those of the authors and not necessarily those of the Federal Highway Administration and/or those of the state highway departments.

REFERENCES

1. Specifications for the Design and Construction of Structural Supports for Highway Signs. American Association of State Highway Officials, 1968.
2. Priest, H. M., and Gilligan, J. A. Design Manual for High-Strength Steels. United States Steel Corporation, 1954.
3. AISC Steel Construction Manual—Specifications for Design, Fabrication and Erection of Structural Steel for Buildings. Sixth edition, American Institute of Steel Construction, 1964.
4. Krefeld, W. J., Butler, D. J., and Anderson, G. B. Welded Cantilever Wedge Beams. Supplement to the Welding Journal, March 1959.
5. Timoshenko, S. P., and Gere, J. M. Theory of Elastic Stability. Second edition, McGraw-Hill Book Company, New York, 1961.
6. Bleich, F. Buckling Strength of Metal Structures. McGraw-Hill Book Company, New York, 1952, p. 151.
7. Guide to Design Criteria for Metal Compression Members. Column Research Council, Engineering Foundation (Johnston, B. G., ed.), Second edition, John Wiley and Sons, New York, 1966.
8. Winter, George. Strength of Slender Beams. ASCE Trans., Vol. 109, 1944, pp. 1321-1358.
9. deVries, Karl. Strength of Beams as Determined by Lateral Buckling. ASCE Trans., Vol. 112, 1947, pp. 1245-1320.
10. Winter, George. Winter on Lateral Buckling. Discussion in ASCE Trans., Vol. 112, 1947, pp. 1272-1276.
11. Gunderson, R. H., and Cetiner, A. Safety Provisions for Support Structures on Overhead Sign Bridges. In A Study of Buckling Stress Formulas, Technical Memo. 605-3, Texas Transportation Institute, College Station, Dec. 1969.
12. AISC Steel Construction Manual—Specifications for Design, Fabrication and Erection of Structural Steel for Buildings. Seventh edition, American Institute of Steel Construction, 1970.

Appendix

NOMENCLATURE

A, A_f, A_w	Areas of the cross section, flange, and web.
a	Distance from neutral axis to point of application of normal load.
b	Width of flange.
c	Distance from neutral axis to edge of beam (usually $d/2$).
d	Depth of beam.
e	Distance from neutral axis to lateral support point.
E	Modulus of elasticity.
F_a, F_b	Maximum allowable stresses in axial and bending respectively (AISC and AASHO)
F_y	Yield point stress.
F.S.	Factor of safety.
f	Calculated or actual stresses.
G	Shearing modulus.
G_A, G_B	End condition parameters used in determining effective lengths (Eq. 11).

I_x, I_y	Moments of inertia about the x and y axes.
K	Torsional rigidity (not equal to the polar moment of inertia for open sections, see Eq. 19).
K_x, K_y, K_z	Effective length factor for bending about the x, y, and z axes.
$\frac{K_y L}{r_y}$, $\frac{L}{r_{yf}}$, $\frac{Ld}{bt}$	Buckling parameters appearing in the critical stress formulas.
L	Unsupported length.
M_0	Applied end moment.
P	Applied point load.
R	Stress reduction factor for tapered beams.
r_x, r_y, r_z	Radii of gyration about the x, y, and z axes.
r_{yf}	Radius of gyration of one flange plus one-sixth the area of the web.
t_f, t_w	Thickness of flange and web.
x, y, z	Coordinate axes.
α	Taper parameter.
δ	Displacement.

Subscripts

a	Refers to axial stress.
b	Refers to bending stress.
cr	Refers to critical stress.
f, w	Denotes the flange and web.
x, y, z	Refers to the x, y, and z axes.
0, 1	Denotes support point and end point on a tapered beam.
$\doteq$	Approximately equal to.

IMPACT RESPONSE OF OVERHEAD SIGN BRIDGES MOUNTED ON BREAKAWAY SUPPORTS

J. E. Martinez, R. M. Olson, and E. R. Post, Texas A&M University

Modern roadways must employ signs that relay information to the motoring public in an efficient manner. The overhead sign bridge (OSB) is often used for this purpose, and collisions with these massive structures have caused serious injuries and fatalities as current installations do not employ safety features that limit impact forces incurred during a collision. This paper presents the general design considerations and the results of the mathematical simulation of vehicle collision with overhead sign bridges mounted on breakaway supports. The results were obtained through the use of a mathematical model verified by seven full-scale crash tests. A comparison of model and test results is shown in the report and indicates good agreement. The study was performed on a high-speed electronic computer, and its findings and the results of the crash tests may be summarized as follows:

1. The application of the breakaway concept to the supports of an overhead sign bridge is feasible.
2. The prototype truss possessed the ability to withstand the torsional loads imparted to it by the rotating support, and the structure as a whole remained stable under the impact forces.
3. Vehicle-velocity changes and deceleration rates increase as breakaway base and upper-shear connection resistances increase.
4. Occupants of small to medium-size vehicles could possibly suffer injury in a collision with the prototype support.
5. Larger vehicles were not severely damaged in collisions with the prototype support.

MANY modern highways employ overhead sign bridges in order to relay information to the motorist in a clear and concise manner. These large and massive structures constitute a safety hazard for the motorist as present installations are not equipped with safety devices that limit the impact forces which a vehicle experiences during a collision. Consequently, collisions with the supports of overhead sign bridges have caused serious injuries and fatalities to vehicle occupants.

The relocation of the support posts offers a solution to the problem. This, however, is usually not economically feasible and other means must be employed in order to eliminate the safety hazard. A concept that has already shown considerable merit when applied to roadside signs and luminaire support structures is the breakaway support which, upon impact, disengages the post from the foundation. Such a concept may be applied to an overhead sign bridge but regard must be given to the possibility of the structure, after impact, falling on the highway and causing an unsafe condition for motorists.

In order to develop a concept into a design that can be utilized under field conditions, it is necessary to investigate its behavior for a variety of cases. For the problem in question this entails evaluation of the effects of different support resistances, and various vehicular weights and impacting velocities. To analyze the different situations a large number of full-scale crash tests may be conducted or else a mathematical model

Sponsored by Committee on Traffic Safety Barriers and Sign, Signal and Lighting Supports and presented at the 50th Annual Meeting.

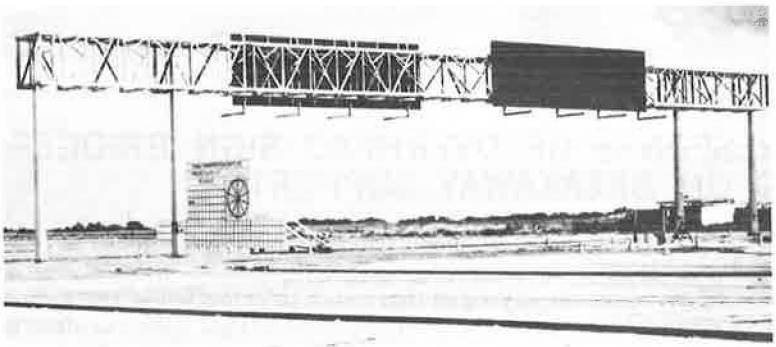

Figure 1. Prototype OSB with four breakaway supports.

that will predict the behavior of the system may be developed. The study described in this paper was carried out on a high-speed computer with the aid of a mathematical model verified by seven full-scale crash tests performed on the prototype overhead sign bridge shown in Figure 1. The model permitted the investigation of a large number of cases and circumvented the high cost associated with performing numerous crash tests.

THE PROTOTYPE OVERHEAD SIGN BRIDGE

The prototype OSB with four breakaway supporting columns is shown in Figure 1. Except for minor modifications, this structure is essentially the same as the preliminary design of Hawkins (1) and is meant to represent a very large OSB structure which might be constructed on modern highways.

The structure under consideration has an overall length of 140 ft. The truss, which is 6 ft in width and depth, is supported by two breakaway exterior and interior columns spaced 20 ft apart. The 100-ft middle section of the structure is of sufficient length to span a four-lane divided highway having standard 12-ft lanes and shoulders, a median width of 18 ft, and a distance of 5 ft from the shoulder edge to the interior columns. The OSB is structurally adequate to resist dead loads and a 100-mph wind load with all four columns in place, whereas, when one of the four columns is disengaged from its foundation, the structure adequately resists dead loads and a wind load of 50 mph.

In order to satisfy the condition for a sign area of 650 sq ft (325 sq ft above travel lanes in each direction) which exceeds the sign area of the majority of contemporary installations, breakaway columns weighing nearly 1,500 lb, were needed. These columns have an overall height of approximately 26½ ft above the slip base and were fabricated from a 100,000-psi heat-treated constructional alloy steel (ASTM 514) and tapered in both the flanges and web. Each column was designed to clear a colliding vehicle and rotates about its own $1^{7}/_{16}$-in.-diameter stainless-steel pin connection following the release of the breakaway base connection and the fracturing of four ½-in. A307 bolts in the upper connection. A close-up view of the column connections is shown in Figure 2.

Following the initial 20-mph pilot test, three important features were incorporated into the existing design. They included:

1. The fastening of steel pipe sections to the lower chord members of the truss (Fig. 3) in order to distribute the impact forces and minimize the possibility of serious damage to the truss due to the impact of the rotating column support.
2. The installation of two horizontal angles, which are visible in Figure 3 at approximately middepth of the truss and on each side of the column, in order to guide the flexible column during an angle collision and prevent the column from damaging the vertical truss members.
3. The placing of a thin sheet-metal "keeper plate" between the slip base plates of the column and the stub post as shown in Figure 2c. This was done to eliminate the possibility of the breakaway columns "walking" off their foundation stub posts during vibrations set up by wind and vehicle traffic.

FORMULATION OF PROBLEM

The structure under consideration is shown in Figure 1 and is comprised of approximately 400 members. The solution for the response of this structure subjected to some loading condition requires solving a large number of simultaneous equations; and, even with the facilities of an IBM 360/65 computer having a core capacity of 100 k words, it is usually necessary to employ outside storage facilities in order to perform the static analysis of the structure. An elastic dynamic analysis considering the entire overhead sign bridge not only adds to the information storage difficulties, but makes the computer cost to solve the problem prohibitive. The reason for this is that the solution must be carried out numerically and the response must be followed for a considerable length of time. Consequently, it was decided to employ three mathematical models to describe the behavior of the structure.

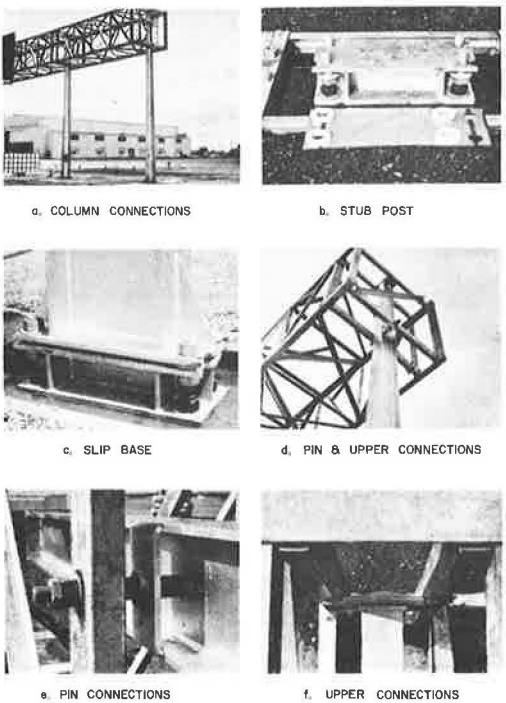

Figure 2. OSB column connections.

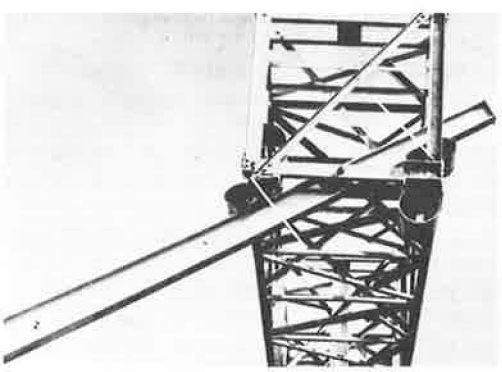

Figure 3. Detail of OSB impact attenuator device.

DISCUSSION OF MATHEMATICAL MODELS

Dynamic Model of Supporting Column

This model assumed the supporting column to be a rigid body having only an angular degree of freedom and being hinged at the truss connection, and idealized the colliding vehicle as a single-degree-of-freedom spring-mass system. This idealized system along with the forces that are taken to act on it is shown in Figure 4.

The forces F_F and F_T in Figure 4 represent shear resistances offered by the base connection and the upper connection to the truss respectively, whereas the force F_S represents the vehicular impact force. A detailed discussion of these forces along with the governing differential equations of motion and the numerical procedure employed to solve them is presented elsewhere (2).

Static Space Truss Model

This model was developed for the purpose of analyzing the overhead sign bridge as a three-dimensional structure under the simultaneous action of weight and wind loads. The effect of the impact force caused by a vehicular collision on the support was considered statically.

The space truss analysis was based on the matrix displacement method of structural analysis and considered the structure to be an assemblage of six-degree-of-freedom truss finite elements. This approach is well established in the literature (3, 4, 5), which also contains a typical element and its stiffness matrix (5, p. 279) and a more complete discussion of this model (2).

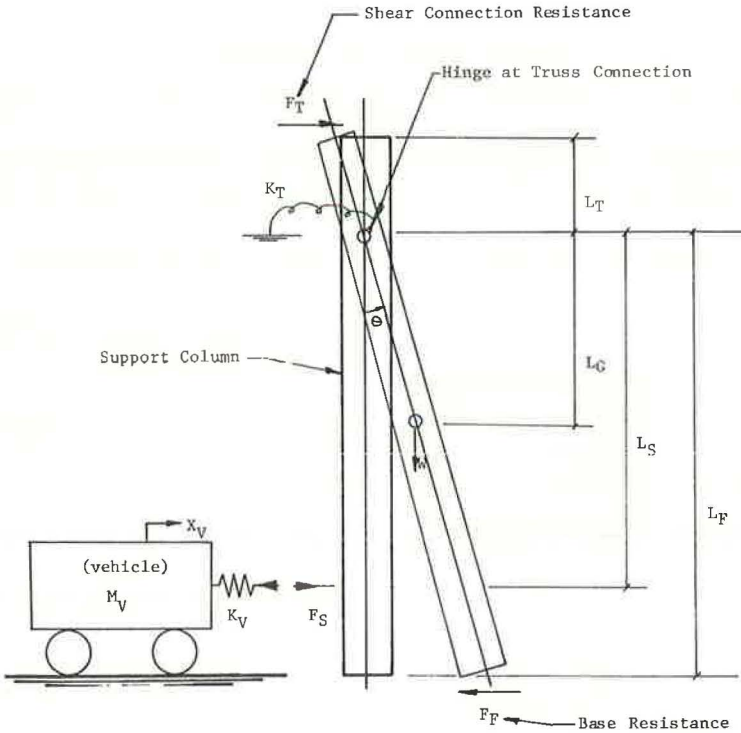

Figure 4. Vehicle and support column idealization.

Torsional Model

A preliminary torsional analysis of the truss portion of the overhead sign bridge has been performed by dividing the structure into substructures and employing static test data obtained from field tests performed at the Texas Transportation Institute on the prototype sign bridge (6). The data permitted the use of realistic stiffness properties in developing a finite element model that circumvented the use of a computer.

The entire structure was subdivided into the substructures shown in Figure 5a which produced the idealized model shown in Figure 5b. For the mathematical modeling, it was assumed that either inner or outer column supports could be struck by a vehicle, but not simultaneously.

Based upon results presented elsewhere (6), values of 750 ft-kips/deg and 79 ft-kips/deg were used for the column pivot stiffness and a 20-ft section of truss respectively. The analysis was conducted by allowing the column supports to offer a resistance only while the shear connection was effective. Empirical values obtained for the torque and the rotation (6) revealed that it was realistic to assume failure at a shear connection when a column bending moment of 230 ft-kips was developed at a point directly below the pivot.

Assuming a collision with an outer support and a shear connection failure at an adjacent inner support produces the model shown in Figure 6a. A further shear-connection failure results in the model depicted in Figure 6b.

It should be emphasized that inelastic action has been precluded in establishing this preliminary model. Under actual field conditions this is not necessarily true and thus the truss may be capable of absorbing more energy than is indicated by this analysis and shown in Figure 7. However, it is felt that the analysis produces energy values that are indicative of what the structure will contain if realistic stiffness coefficients

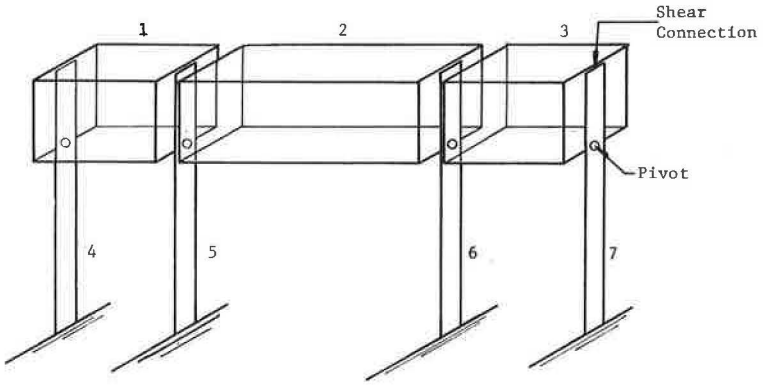

a. Representation by series of substructures

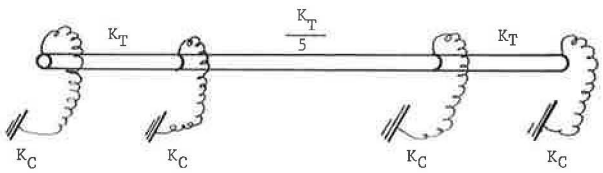

*K_T = Truss Stiffness for 20ft. Section.
*K_C = Stiffness of Column Support.

b. Idealized torsion model

Figure 5. Overhead sign bridge.

can be determined. Significant variations in the empirical values used in this analysis could produce a sizeable change in the energy-absorbing capability of the truss.

It should be noted that the accuracy of the results obtained with this model is dictated by the values of the stiffness coefficients that are employed. To date, a good correlation between stiffness coefficients obtained from the static space truss model and the test results (6) has not been possible. This can partially be attributed to the manner in which the boundary conditions are imposed on the model. A study to obtain a model that will accurately predict these coefficients appears to be extremely worthwhile but has presently not been undertaken.

Correlation—Space Truss

Presently, the information obtained from the static space truss model has been mostly limited to checking out the design of the prototype truss for wind and gravity loads, and the results obtained for the deflections and stresses indicate that the design is adequate. The model may also be employed to determine stiffness coefficients for the truss; however, as mentioned previously, adequate correlation between model and field test results has not been obtained. A stability analysis of the truss is not beyond the scope of the model and this capability could be incorporated into the existing computer code if such an analysis became warranted.

The results obtained from the torsional model are based on the limited amount of test data available and may be summarized by the torque-rotation curve shown in Figure 7. This curve shows that the truss is capable of absorbing approximately 145 ft-kips of energy and rotating through 25 deg before failure at the upper shear connection C occurs. It is felt that this amount of energy-absorbing capability is sufficient to cope

with a collision by a 5,000-lb vehicle traveling at 60 miles per hour and having an approach angle of zero.

Correlation—Support

In order to validate the dynamic model of the supporting column, the results obtained from the computer solution were compared with the results obtained from seven full-scale crash tests performed by the Texas Transportation Institute; comparisons are given in Tables 1 and 2. The tables give a summary of crash test data and compare test results with mathematical simulation predictions for the response of the structure when subjected to vehicular impact. These values offer a comparison of the model with crash test data for various situations and provide information that illustrates the limitations of the results.

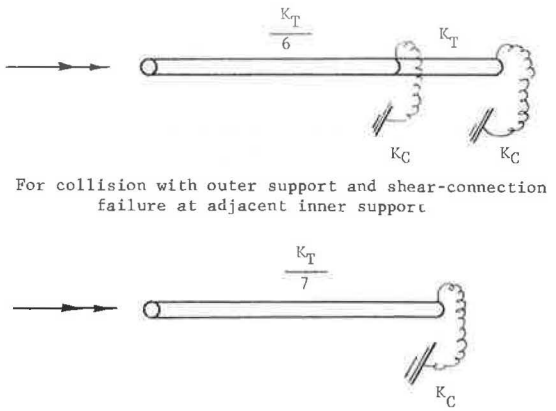

a. For collision with outer support and shear-connection failure at adjacent inner support

b. For collision with outer support and shear-connection failure at both inner supports

Figure 6. Torsion models of overhead sign bridge.

Table 1 gives a comparison of the vehicular velocity changes, deceleration rates, and time the post and vehicle are in contact, whereas Table 2 gives values obtained for the maximum post penetration and comments on the rotation of the support.

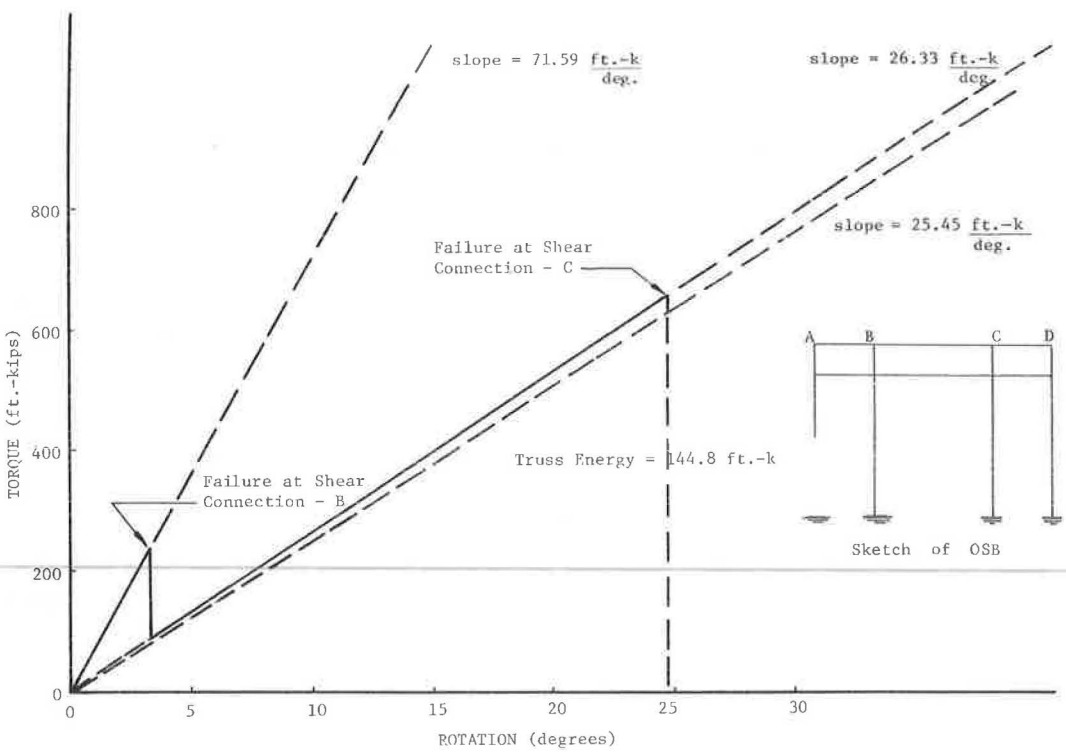

Figure 7. Torque-rotation curve for collision with outer support.

TABLE 1
SUMMARY OF CRASH TEST DATA AND MODEL SIMULATION

Test Conditions						Comparison of Results					
						Change in Vehicle Velocity (mph)		Time Post and Vehicle Were in Contact (sec)		Average Deceleration (g)	
Test Number	Date of Test	Year, Make, and Type of Vehicle	Vehicle Weight (lb)	Vehicle Approach Angle (deg)	Impact Velocity (mph)	Test	Model	Test	Model	Test	Model
605-A	09-23-69	1963 Ford 2-door sedan	3,960	0	25.7	5.4	5.9	0.091	0.082	2.9	2.9
605-B	12-11-69	1959 Simca 4-door sedan	2,100	0	44.0	14.8	16.2	0.080[a]	0.139	8.7	5.3
605-C	12-18-69	1963 Ford 4-door sedan	4,090	0	46.5	9.1	9.3	0.080	0.099	5.7	4.3
605-D	02-03-70	1962 Cadillac 4-door sedan	4,880	0	54.0	9.0	9.1	0.080	0.087	4.2	4.7
605-E	02-09-70	1963 Ford 4-door sedan	3,920	15	28.6	7.2	7.0	0.085	0.095	4.1	3.4
605-F	02-17-70	1959 Borgward 2-door sedan	2,350	15	52.0	13.6	16.7	0.119	0.130	5.8	5.8
605-G	04-07-70	1962 Ford 2-door sedan	3,950	15	50.1	10.2	10.4	0.059	0.093	7.9	5.1

[a]Time during which breakaway components were activated. Vehicle snagged lower end of support post, was lifted and pulled to a stop, wedged between support post and the ground.

The crash test data were obtained from electronic instrumentation and high-speed film, and these data have been found to agree reasonably well with the computer simulation. Some of the differences between test results and mathematical simulation can be attributed to data reduction and analysis techniques. For example, values of the contact time and vehicle translation during contact are obtained by observation of the high-speed film and it is difficult to establish precisely the time when contact is lost. The relative precision of test results is being studied by other members of the Texas Transportation research team and is reported elsewhere (6).

The first four tests were head-on impacts, whereas with the last three the vehicular approach was at an angle of 15 deg. In all cases, head-on impact was assumed by the mathematical model without any appreciable difference between model and test results.

From the values shown in Tables 1 and 2, it is evident that collisions by medium-weight vehicles traveling in excess of 25 mph cause the support post to strike the truss.

TABLE 2
SUMMARY OF CRASH TEST DATA AND MODEL SIMULATION

Test Conditions					Comparison of Results			
					Maximum Post Penetration (ft)		Remarks	
Test Number	Year, Make, and Type of Vehicle	Vehicle Weight (lb)	Vehicle Approach Angle (deg)	Impact Velocity (mph)	Test	Model	Test	Model
605-A	1963 Ford 2-door sedan	3,960	0	25.7	0.96	0.97	Post hits truss	Post hits truss E_k = 3.1 ft-kip[b]
605-B[a]	1959 Simca 4-door sedan	2,100	0	44.0	1.75	2.15	Post hits truss	Post hits truss E_k = 19.1 ft-kip[b]
605-C	1963 Ford 4-door sedan	4,090	0	46.5	1.25	1.63	Post hits truss	Post hits truss E_k = 38.5 ft-kip[b]
605-D	1962 Cadillac 4-door sedan	4,880	0	54.0	1.50	1.60	Post hits truss	Post hits truss E_k = 62.86 ft-kip[b]
605-E	1963 Ford 4-door sedan	3,920	15	28.6	0.85-1.1	1.13	Post hits truss	Post hits truss E_k = 6.5 ft-kip[b]
605-F	1959 Borgward 2-door sedan	2,350	15	52.0	1.5-1.8	2.30	Post hits truss	Post hits truss E_k = 37.0 ft-kip[b]
605-G	1962 Ford 2-door sedan	3,950	15	50.1	1.60	1.76	Post hits truss	Post hits truss E_k = 48.9 ft-kip[b]

[a]Vehicle snagged support base and was lifted by it.

[b]Angular kinetic energy of post.

In tests conducted to date, the contact made with the truss by the support has not damaged the truss. This can be attributed partially to the energy-absorbing, load-distributing devices attached to the truss, as shown in Figure 3. However, it is possible for a high-speed collision to cause severe local damage to truss members unless adequate load-distributing devices are installed on the truss. To provide a satisfactory design, such devices must allow the support to rotate through an angle large enough to clear the vehicle and yet be able to absorb a sufficient amount of the rotational kinetic energy of the support. A device made from 12-in.-diameter, $^3/_8$-in.-wall-thickness pipe was installed on the truss. In addition, 4 in. by 4 in. by 12 in. angles were installed to prevent the upper portion of the support from contacting the vertical truss members. These and other design details are discussed elsewhere (7).

The average deceleration rates obtained from the crash tests agree quite well with the results obtained from the computer model. An unexpected incident occurred in Test 605-B; in this test, the vehicle snagged the support post and was lifted by it. Contact between the vehicle and the support was never lost. The average vehicle deceleration is based on film observation (Table 1).

The agreement in values obtained for the maximum post penetration is very satisfactory (Table 2). The softer front ends of the lightweight vehicles permit a larger post penetration than do the sturdier medium- and heavy-weight vehicles; however, all penetrations are small when compared with similar penetration by a fixed post.

In an earlier study (8), several vehicles were crashed into a fixed support, and maximum post penetrations were recorded. For similar conditions, post penetration by a fixed post was much greater than that measured in the current series of tests on a breakaway support. For example, the fixed-post penetration into a 1959 Simca 4-door sedan, traveling 45 mph was 4.25 ft compared with 1.75-ft penetration by the breakaway support in the current series; and a 1959 4-door Cadillac, traveling 44 mph was penetrated 4.50 ft by the fixed post compared with 1.50 ft in the current tests. These comparisons are indicative of the relative severity of collisions with a fixed support and with the breakaway support.

The comparison shown for the seven tests reveals that good agreement exists between the computer model and the field tests. Further, the feasibility of the breakaway concept for the supports of an overhead sign bridge has been demonstrated.

PARAMETER STUDY

The parameter study revealed that lower vehicular velocity changes and deceleration rates may be expected for lower values of the base and shear connection resistances (2). However, due to the massiveness of the support, the major portion of the change in the vehicle response can be attributed to the inertia of the column. This is particularly true for the higher impact velocities. The decrease in the resistance offered by the column also normally results in a higher kinetic energy being imparted to the support. This produces a larger rotation of the support and could cause interference between the truss and the support. The impact on the truss by the column can conceivably cause damage to the truss.

The vehicle deformation is likewise primarily caused by the large mass of the support. For a given base and shear-connection resistance, the vehicle deformation increases with an increase in the impact velocity and reaches a maximum of 2.80 ft for the case of the 2,000-lb vehicle having an impact velocity of 60 mph (Table 5). It should be noted that the model assumes the vehicle spring constant to be equal to ten times the vehicle weight and consequently the lighter vehicle has a relatively soft spring which produces larger deformations.

Light- and medium-weight vehicles experience a secondary collision with the support when it is impacted at a velocity of 15 mph (Table 3). These collisions should be interpreted as hazardous because the secondary collision will occur in the area of the passenger compartment and could cause injury to the occupants. The remainder of the cases presented disclose that the post always clears the vehicle. This is desirable from the standpoint of circumventing a secondary impact; however, the vehicular velocity changes may be excessive or the vehicle may impart such a large amount of energy to the support that damage to the truss is produced.

TABLE 3

PARAMETER STUDY—RESULTS FOR HEAD-ON COLLISION AT A VEHICULAR VELOCITY OF 15 MPH AND 22 K SHEAR-CONNECTION RESISTANCE

Vehicle Weight (lb)	Base Resistance (kips)	ΔV (mph)	Average g	Contact Time (sec)	Maximum Post Penetration (ft)	Comments
2,000	0	6.19	1.94	0.146	0.77	Post hits top of vehicle
2,000	2	7.15	2.26	0.145	0.84	Post hits top of vehicle
2,000	7	12.72	5.01	0.116	1.01	Post hits hood of vehicle
2,000	10	15.0	5.6	0.084	1.03	Vehicle was stopped
3,500	0	3.7	1.6	0.106	0.60	Post clears vehicle
3,500	2	4.1	1.7	0.111	0.62	Post hits top of vehicle
3,500	7	5.6	2.4	0.104	0.75	Post hits top of vehicle
3,500	10	7.1	3.4	0.096	0.80	Post hits top of vehicle
5,000	0	2.8	1.7	0.076	0.50	Post clears vehicle
5,000	2	3.0	1.7	0.079	0.50	Post clears vehicle
5,000	7	3.7	2.1	0.082	0.60	Post clears vehicle
5,000	10	4.5	2.5	0.078	0.64	Post clears vehicle

It has been suggested in the literature (9) that vehicular velocity changes in excess of 11 mph should be avoided if a hazardous condition that could cause injury to the vehicle occupants is to be prevented. Thus, based on this criterion, hazardous collisions occur when lightweight, slow-moving vehicles or light- and medium-weight vehicles traveling at high speeds impact the column support. In all these cases the vehicular velocity changes exceed 11 mph and reach a maximum of 21 mph for a case shown in Table 5.

The values of E_k given in Tables 3 through 6 represent the angular kinetic energy of the support at the instant it has rotated through an angle large enough to cause the support and the truss to interfere. This condition was taken to occur at a support rotation of 81.5 deg. These values can become quite large as the impact velocity is increased, and for the higher velocities an energy absorber should be placed on the truss. This absorber would take in some of the angular kinetic energy of the support and keep the truss from having to cope with such a large amount of energy.

TABLE 4

PARAMETER STUDY—RESULTS FOR HEAD-ON COLLISIONS AT A VEHICULAR VELOCITY OF 30 MPH AND 22 K SHEAR-CONNECTION RESISTANCE

Vehicle Weight (lb)	Base Resistance (kips)	ΔV (mph)	Average g	Contact Time (sec)	Maximum Post Penetration (ft)	Comments
2,000	0	10.26	3.38	0.139	1.36	Post hits truss E_k = 1.84 ft-kip
2,000	2	10.8	3.48	0.142	1.42	Post hits truss E_k = 1.40 ft-kip
2,000	7	12.4	3.86	0.147	1.58	Post hits truss E_k = 0.08 ft-kip
2,000	10	13.96	4.37	0.146	1.70	Post clears vehicle
3,500	0	6.5	2.90	0.103	1.07	Post hits truss E_k = 7.13 ft-kip
3,500	2	6.8	3.10	0.099	1.10	Post hits truss E_k = 7.66 ft-kip
3,500	7	7.4	3.00	0.112	1.20	Post hits truss E_k = 6.03 ft-kip
3,500	10	7.8	3.10	0.113	1.20	Post hits truss E_k = 5.82 ft-kip
5,000	0	4.9	2.90	0.078	0.91	Post hits truss E_k = 11.33 ft-kip
5,000	2	4.96	2.70	0.083	0.93	Post hits truss E_k = 10.33 ft-kip
5,000	7	5.3	2.90	0.085	0.99	Post hits truss E_k = 10.16 ft-kip
5,000	10	5.7	3.08	0.084	1.00	Post hits truss E_k = 10.68 ft-kip

TABLE 5

PARAMETER STUDY—RESULTS FOR HEAD-ON COLLISION AT A VEHICULAR VELOCITY OF 60 MPH AND 22 K SHEAR-CONNECTION RESISTANCE

Vehicle Weight (lb)	Base Resistance (kips)	ΔV (mph)	Average g	Contact Time (sec)	Maximum Post Penetration (ft)	Comments
2,000	0	19.00	4.68	0.185	2.60	Post hits truss E_k = 48.86 ft-kip
2,000	2	19.20	4.63	0.189	2.60	Post hits truss E_k = 47.76 ft-kip
2,000	7	20.20	5.30	0.174	2.70	Post hits truss E_k = 46.82 ft-kip
2,000	10	21.10	6.10	0.157	2.80	Post hits truss E_k = 46.57 ft-kip
3,500	0	12.30	5.00	0.111	2.00	Post hits truss E_k = 69.12 ft-kip
3,500	2	12.40	4.80	0.116	2.08	Post hits truss E_k = 67.79 ft-kip
3,500	7	13.00	5.70	0.103	2.10	Post hits truss E_k = 71.14 ft-kip
3,500	10	13.20	5.50	0.110	2.20	Post hits truss E_k = 68.81 ft-kip
5,000	0	9.20	5.07	0.083	1.70	Post hits truss E_k = 83.22 ft-kip
5,000	2	9.30	5.04	0.084	1.77	Post hits truss E_k = 82.41 ft-kip
5,000	7	9.50	4.80	0.090	1.80	Post hits truss E_k = 79.49 ft-kip
5,000	10	9.90	5.70	0.080	1.80	Post hits truss E_k = 86.28 ft-kip

The angular kinetic energy values (E_k) presented in Tables 2 through 6 are taken at an instant when the support has rotated through an angle large enough to cause the truss and the support to interfere. They reveal that, according to the mathematical model, the relationship between angular kinetic energy of the support and vehicle impacting velocity is almost linear for a given vehicular weight.

Table 6 presents the results from some extreme cases. Here, 10,000-lb and 20,000-lb vehicles have been selected and the base and shear-connection resistances have been taken as 10 k and 22 k respectively. The 10,000-lb vehicle was assumed to have a height of 11 ft and a length of 27 ft, whereas the 20,000-lb vehicle has 11 ft and 36 ft values. The vehicular spring constant was taken as 100,000 lb/ft for both vehicles.

TABLE 6

PARAMETER STUDY—RESULTS FOR HEAD-ON COLLISIONS BY 10,000- AND 20,000-LB VEHICLES

Vehicle Weight (lb)	Vehicle Velocity (mph)	ΔV (mph)	Average g	Contact Time (sec)	Maximum Post Penetration (ft)	Comments
10,000	15	2.20	2.0	0.049	0.040	Post hits vehicle
10,000	30	2.90	2.5	0.053	0.070	Post hits truss E_k = 17.8 ft-kip
10,000	45	4.10	3.5	0.053	1.00	Post hits truss E_k = 55.3 ft-kip
10,000	60	5.40	4.8	0.051	1.30	Post hits truss E_k = 111.8 ft-kip
20,000	15	1.20	1.6	0.033	0.23	Post hits truss E_k = 4.0 ft-kip
20,000	30	1.77	2.6	0.031	0.50	Post hits truss E_k = 36.9 ft-kip
20,000	45	2.10	1.9	0.051	1.00	Post hits truss E_k = 64.9 ft-kip
20,000	60	2.70	2.3	0.055	1.30	Post hits truss E_k = 114.6 ft-kip

Note: These results are for a base resistance of 10 k and a shear-connection resistance of 22 k.

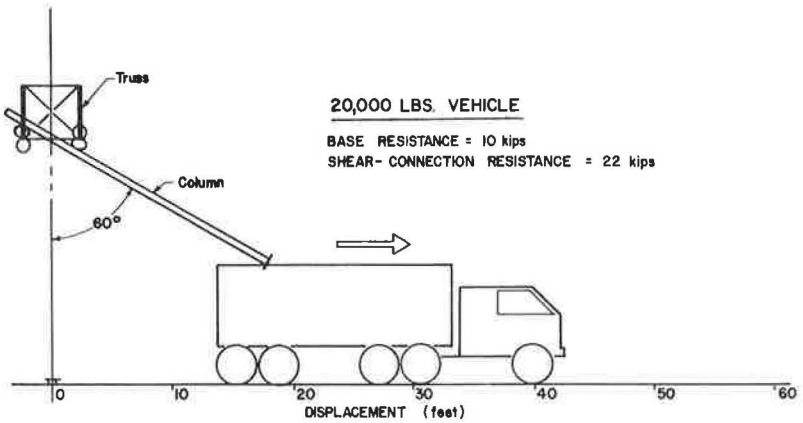

Figure 8. Column response for impact at 30 mph (simulated head-on impact).

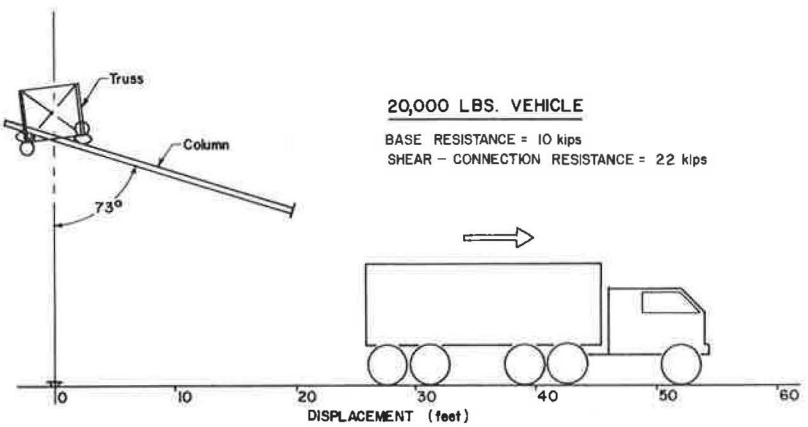

Figure 9. Column response for impact at 60 mph (simulated head-on impact).

The results in Table 6 reveal that the two 15-mph cases and the 10,000-lb vehicle traveling at 30 mph encounter a secondary collision with the support. Figure 8 shows a case where a secondary collision is encountered, whereas Figure 9 shows an example of a support clearing the vehicle.

The energy values, E_k, to which the truss is subjected when struck at high impact speeds are quite large, and indicate that, as the vehicle velocity is increased, the effect of the vehicle mass on the angular kinetic energy of the support becomes less significant. For example, at an impact velocity of 60 mph the angular kinetic energy of the support, at the instant it encounters the truss, is only increased from 111.8'k to 114.6'k as the vehicle mass is increased from 10,000 to 20,000 lb. This fact may be used to set up design criteria for energy absorbers that could be placed on the truss.

CONCLUSIONS

The general conclusions listed in this section are based on the mathematical models developed, observations of full-scale crash tests, and the results of the parameter study.

They may be summarized as follows:

1. The application of the breakaway concept to the supports of an overhead sign bridge is feasible.
2. The prototype truss possessed the ability to withstand the torsional loads imparted to it by the rotating support and the structure as a whole remained stable under the impact forces.
3. Vehicle velocity changes and deceleration rates increase as breakaway base and upper shear-connection resistances increase.
4. Vehicle velocity changes, deceleration rates, and vehicle damage resulting from a collision increase as column support weight increases.
5. Occupants of small to medium-size vehicles may suffer injury in a collision with the prototype support.
6. Larger vehicles are not severely damaged in collisions with the prototype breakaway support.
7. The damage to vehicles in impacts with breakaway supports was appreciably less than that to similar vehicles which struck a fixed support post.

ACKNOWLEDGMENT

The research study presented in this paper was supported by the highway departments of the states of Alabama, Arkansas, Connecticut, Florida, Georgia, Hawaii, Kentucky, Louisiana, Maryland, Michigan, Mississippi, Montana, Nebraska, New Hampshire, New Mexico, Rhode Island, South Dakota, Tennessee, Texas, West Virginia, Wyoming, and the District of Columbia. It was administered by the Department of Transportation, Federal Highway Administration, under Contract No. FH-11-7032.

The opinions, findings, and conclusions expressed herein are those of the authors and not necessarily those of the Federal Highway Administration and/or those of the state highway departments.

REFERENCES

1. Hawkins, D. L. Preliminary Calculations for a Prototype Overhead Sign Bridge With Breakaway Supports. Dated October 1965, and forwarded to the Texas Transportation Institute for consideration.
2. Martinez, J. E., Jumper, J. J., and Baskurt, F. Y. Safety Provisions for Support Structures on Overhead Sign Bridges—Mathematical Simulation and Correlation. Technical Memorandum 605-2, Texas Transportation Institute, Texas A&M University, College Station, December 1969.
3. Przemieniecki, J. S. Theory of Matrix Structural Analysis. McGraw-Hill Book Co., Inc., New York, 1968.
4. Martin, H. C. Introduction to Matrix Methods of Structural Analysis. McGraw-Hill Book Co., Inc. New York, 1966.
5. Gere, J. M., and Weaver, W. Analysis of Framed Structures. D. Van Nostrand Co., Inc., Princeton, N. J., 1965.
6. Ivey, D. L., Olson, R. M., Buth, E., and Hirsch, T. J. Safety Provisions for Support Structures on Overhead Sign Bridges—Testing Program. Technical Memorandum 605-4, Texas Transportation Institute, Texas A&M University, College Station, May 1970.
7. Post, E. R., Garner, C. P., and Olson, R. M. Safety Provisions for Support Structures on Overhead Sign Bridges—Design, Analysis and Construction. Technical Memorandum 605-1, Texas Transportation Institute, Texas A&M University, College Station, December 1969.
8. Edwards, T. C., Hirsch, T. J., and Olson, R. M. Break-Away Sign Support Structures. Volume 1, Final Report on Highway Sign Support Structures, Project HPR-2(104), Texas Transportation Institute, Texas A&M University, College Station, July 1967, p. 8:103.
9. Patrick, L. M., et. al. Knee, Chest, and Head Impact Loads, Proceedings of the 11th Stapp Car Crash Conference. Anaheim, Calif., October 10-11, 1967, p. 116.

BREAKAWAY OVERHEAD SIGN BRIDGES, CRASH TESTING

D. L. Ivey, R. M. Olson, C. E. Buth, and T. J. Hirsch,
Texas Transportation Institute, Texas A&M University; and
D. L. Hawkins, Texas Highway Department

This paper describes ten vehicle crash tests that were conducted on an overhead sign bridge. The purpose of these tests was to determine the feasibility of large breakaway supports for these bridges. The behavior of the overhead sign bridge when subjected to vehicle impact loads also was determined during this study. The vehicles ranged in weight from 2,100 to 5,170 lb. Impact speeds ranged from 25.7 to 75.3 mph. These tests indicate that the breakaway safety features of the overhead sign bridge will greatly reduce the forces on impacting vehicles.

•THE ERECTION of the prototype overhead sign bridge with breakaway supports was completed on September 8, 1969. A testing program was begun to determine and evaluate the forces imposed on vehicles colliding with the breakaway supports and to observe and analyze the behavior of the prototype structure under a variety of collision conditions. Ten vehicle crash tests were conducted on the prototype structure shown in Figure 1. Table 1 gives a summary of crash test results. Deceleration forces were measured by accelerometers mounted on the frame of the vehicle.

TEST A

The first vehicle crash test in the development and evaluation program was conducted on September 23, 1969. A 1963 Ford impacted support "A" at a speed of 25.7 mph. The design conditions required that a 28-gage "keeper" plate be installed between the upper

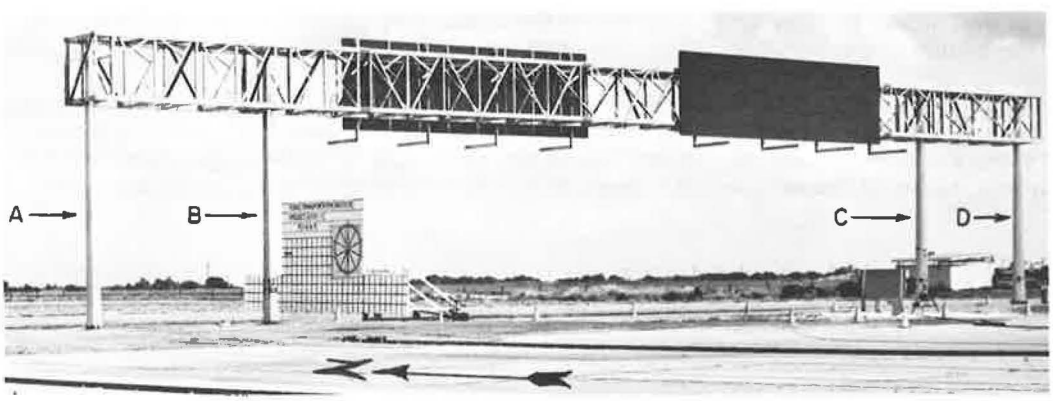

Figure 1. Prototype overhead sign bridge. Supports designated A, B, C, and D.

Sponsored by Committee on Traffic Safety Barriers and Sign, Signal and Lighting Supports and presented at the 50th Annual Meeting.

TABLE 1

SUMMARY OF VEHICLE CRASH TEST RESULTS

Characteristic	Test No.								
	A	B	C	D	E	F	G	H	I
Vehicle make	Ford	Simca	Ford	Cadillac	Ford	Borgward	Ford	Cadillac	Cadillac
year	1963	1959	1963	1962	1963	1959	1962	1961	1962
Vehicle weight, lb	3,950	2,100	4,090	4,880	3,920	2,350	3,950	5,150	5,170
Impact angle, deg	0	0	0	0	15	15	15	0	15
Initial speed, mph[a]	25.7	44.0	46.5	54.0	28.6	52.0	50.1	75.3	72.0
Change in speed, mph[a]	5.4	14.7[b]	8.9	9.0	7.2	13.6	10.2	11.5	11.2
Avg. decel., g (long.)	3.1	9.6	6.7	7.8	3.7	12.2	5.8	6.9	8.8
g (trans)	—	—	—	—	0.1	1.3	0.6	—	0.4
Peak decel., g (long.)	7.4	22.4	19.1	15.1	8.8	30.8	15.3	17.6	22.4
g (trans)	—	—	—	—	3.4	8.7	3.6	—	4.7
Target support	A	B	B	A	B	A	A	A	B
Max. rotation of support, deg[a]	83	65[c]	63	68	65	59	65	77	70
Height of lower end of support at peak of swing, ft[a]	19.5	12.1	11.5	13.1	12.1	10.2	12.1	16.3	13.5
Approx. rotation of truss, deg[a]	2	3	1	9	1	4	8	60	1.6

[a]From film data.

[b]Change in velocity over the period necessary to activate the breakaway component of the support. Vehicle snagged on lower end of support post and was stopped.

[c]Impact load distributors were installed in this and all following tests.

and lower base plates and that the base bolts be tightened to 200 lb-ft (Fig. 2). Preliminary calculations and analysis of the record films led to the conclusion that the bolt keeper plate and base-bolt torque do not affect the vehicle-support behavior. These conditions (28-gage bolt keeper plate and 200 lb-ft base-bolt torque) were established for the remainder of the regular crash test series.

The reaction of the support was predicted by mathematical simulation. The support rotated through 83 deg (observed), allowing the vehicle to pass underneath. Damage to the vehicle was slight as shown in Figure 3. Sequential photographs of the interaction of the overhead sign bridge (OSB) with the test vehicle during the test are shown in Figure 4.

TEST B

In evaluating the breakaway features of the overhead sign bridge and the functioning of the bridge structure, two distinct areas of interaction are apparent: (a) the interaction of the vehicle with the support; and (b) the interaction of the rotating OSB support with the lower chord members of the truss. The first test showed that the interaction of the vehicle with the support leg could be predicted with reasonable accuracy by use of computer simulation. The interaction of the rotating support with the truss then became a matter of major concern. For vehicle velocities greater than 25 mph, the

Figure 2. Details of breakaway base connection.

Figure 3. Vehicle after Test A.

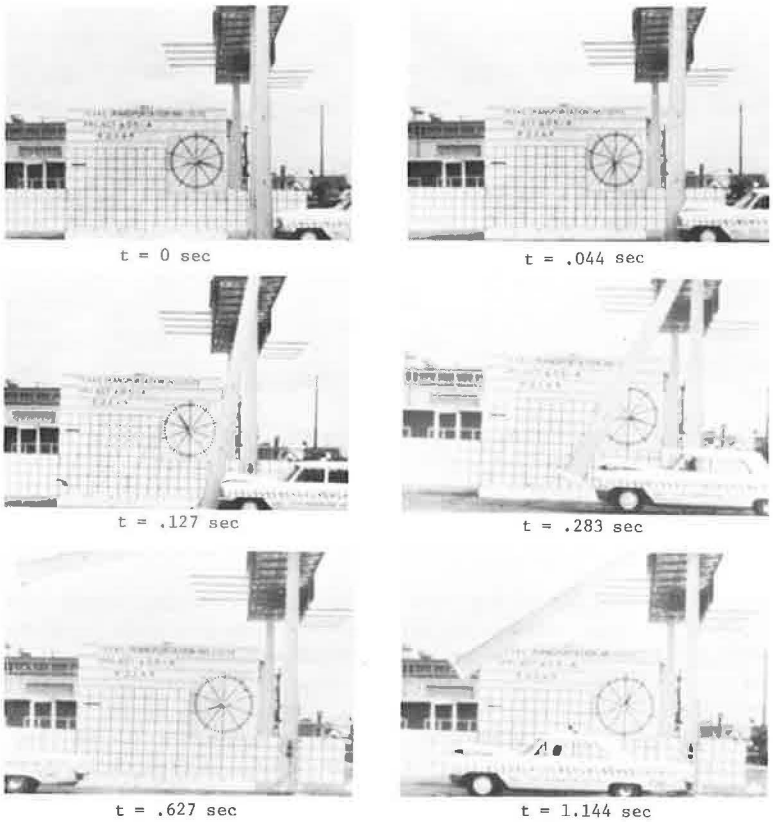

Figure 4. Sequential photographs of Test A.

computer simulation predicted that the support would possess significant kinetic energy when it impacted the lower chords of the truss (1). The protection of the lower chord members by distribution of the impact force and by dissipation of excess energy was carefully considered. To provide the required distribution and dissipation a steel-tube load distributor was designed which could be placed to protect the lower chord members of the truss. Static laboratory and field tests were run to verify the function of these distributors before crash tests were conducted. A close-up of the load distributor before it was placed on the truss is shown in Figure 5, and typical installations on the truss are shown in Figures 6 and 7. Selection of the channel sections was made (a) to provide adequate load distribution to the truss, and (b) to provide a flat bearing surface for the cylindrical tubes during impact loading. The design of the connection provided both conditions, as can be seen in Figure 8. No damage to the lower chord occurred

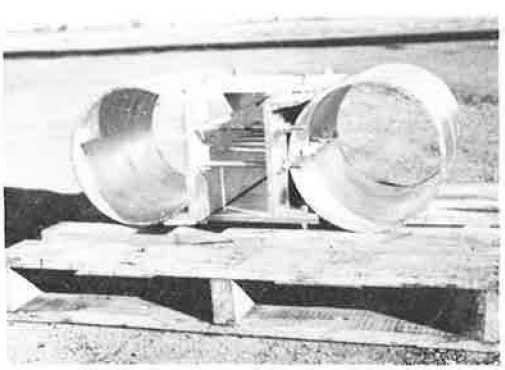

Figure 5. Load distributor (steel tubing with 3/8-in. wall thickness, 12 3/4-in. outside diameter, and 17 in. long).

Figure 6. Load distributor bolted in place on lower truss chord at support A.

Figure 7. Load distributors at support B before Test B.

and the energy absorbers were crushed against the channel sections, as had been anticipated.

On the basis of an analysis of the OSB subjected to torsional loads and the empirical data developed in static load tests (2), the torsional stiffness coefficients for various components of the overhead sign bridge were determined. Using these coefficients, the amount of energy which the truss could be expected to absorb before fracturing connection bolts at the top of all four supports was estimated to be 145 kip-ft. However, it was decided that the validity of this analysis should be tested and that the energy level of the impacting vehicle, and therefore the energy of the subsequently rotating support, should be increased gradually until the dynamic functioning of the tube load distributors and the energy-absorption capability of the OSB were further verified. For this reason, the speed of the impacting vehicle in Test B was increased to 44 mph. A 1959 Simca weighing 2,100 lb was used in this test to ascertain the interaction between the breakaway support and a lightweight, compact vehicle. The truss and support conditions were the same as in Test A, except that support B was the target.

An unexpected incident occurred during Test B: the front of the vehicle was deformed significantly in the collision, remained in contact with the support, and the vehicle was lifted at the front end by the support finally wedging itself between the ground and support in a nearly vertical position. The post penetrated 21 in. toward the engine and the front frame cross member was bent, forcing the two longitudinal frame members to come together, thus clamping the support in a pincer-like action. This pincer-like action prevented the support from springing away from the vehicle after the connections at the base and top of the support broke away. As the support rotated, while maintaining contact with the automobile, the upper base plate elevated, and the slotted projections of this base plate acted as a hook which caught the front end of the vehicle and raised it to the maximum elevation shown at t = 0.781 second in Figure 9.

Close-up views of the front end of the car are shown in Figures 10 and 11. Examination of data from accelerometers indicated that the average deceleration was 9.6 g over 0.068 second. The peak deceleration was 22.4 g occurring at ap-

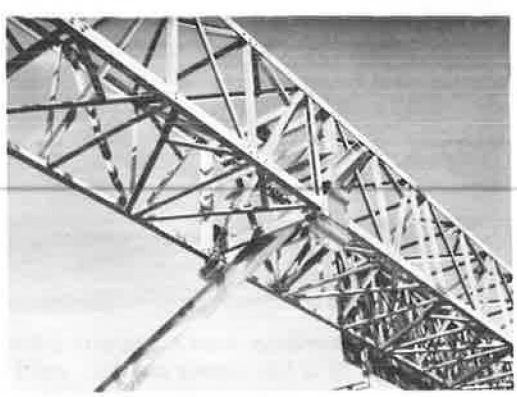

Figure 8. Load distributor at support B after Test B.

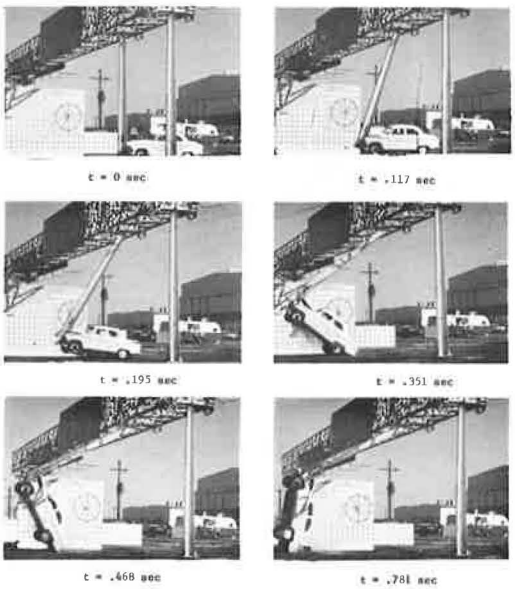

Figure 9. Sequential photographs of Test B.

Figure 10. Vehicle wedged between support and ground (Test B).

proximately 0.050 second. The load distributors functioned as expected, and there was no apparent damage to the truss.

The events and behavior just described resulted in considerable discussion concerning ways to (a) eliminate the "hooking" of automobiles, or (b) determine whether larger automobiles would behave as the small vehicle had. The latter determination took priority and the next test was scheduled without changes to the prototype structure.

Figure 11. Vehicle after Test B.

TEST C

A 1963 Ford weighing 4,090 lb impacted support B head-on at a speed of 46.5 mph, and the vehicle and support interaction was similar to that reported for Test A. The breakaway devices at the base and top of support B performed as anticipated, allowing the support to rotate up and away from the vehicle. During the time from initial vehicle contact until the upper bolts fractured, the truss rotation was approximately 1 deg. The vehicle passed under the support with a clearance of approximately 6 ft. After swinging through an angle of 50 deg, the support made contact with the load distributors and proceeded to crush them until the support rotation had increased to 63 deg. During the crushing of the load distributors, the rotation of the truss was less than 1 deg; thus the steel tubes absorb some energy but function primarily as load distributors.

The average vehicle deceleration was determined to be 6.7 g over 0.064 second, and a peak deceleration of 19.1 g, occurring at t = 0.050 second, was observed on the accelerometer trace. The vehicle's speed was reduced 8.9 mph by the collision. Damage to the vehicle is shown in Figure 12.

It was observed that the truss deflects downward at inner support B following impact, and as a result the support comes to rest at the lower base plate sooner than when an outer support is struck. The conditions following this test are shown in Figure 13. Similar behavior was observed in later tests, and it was found that, when the outer support is struck, the support post continues to swing as a pendulum for several seconds after impact.

Figure 12. Vehicle after Test C.

TEST D

Computer simulation predictions (1) indicated that a head-on collision involving a heavy automobile would produce tolerable damage to the colliding vehicle and the prototype structure. To verify this prediction a 4,880-lb automobile, traveling 54 mph, struck the outer support A. The sign bridge functioned as predicted; vehicle damage was slight as shown in Figure 14, and no structural damage to the truss or support leg was observed. The truss rotation from the time the vehicle contacted the support until the upper connection bolts fractured at support A was less than 1 deg. The maximum rotation of the truss was 9.4 deg as support A rotated upward through 68 deg. During this rotation, the upper connection bolts at support B also fractured. The rotation of the truss at this time is shown in Figure 15 at t = 0.453 second.

Using photographic analysis, the angular velocity of the support was estimated at first contact with the load distributors, and the kinetic energy of the support at this time was determined to be 49.8 kip-ft. An energy of 62.8 kip-ft had been predicted by computer simulation. Under the action of the rotating support, the truss was twisted approximately 9 deg. Using methods described in the Final Report of this study (2), the energy absorbed by the truss was estimated to be 25.8 kip-ft. The change in potential energy of the support from first contact with the load distributors to its maximum elevation was 4.6 kip-ft. The difference between gravitational potential energy plus the energy absorbed by the truss is 19.4 kip-ft, which is the estimated energy absorbed by the load distributors.

Figure 13. Impact area after Test C.

Figure 14. Vehicle after Test D.

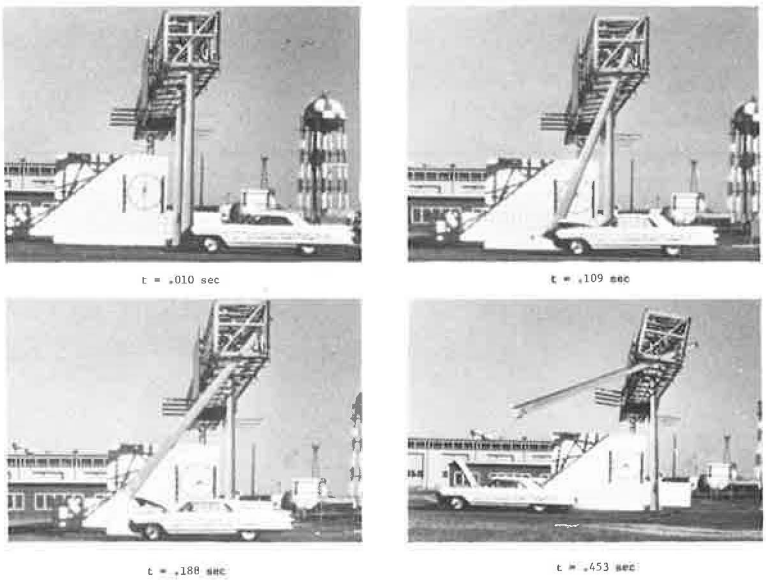

Figure 15. Sequential photographs of Test D.

Laboratory investigations indicated that the load distributors are capable of absorbing 40 kip-ft, and the potential of the OSB to absorb torsional energy is estimated to be 145 kip-ft. Under these conditions the upper connection bolts at support C should fracture.

After consultations with members of the Project Policy Committee and the Technical Subcommittee, it was decided to conduct crash tests at an impact angle of 15 deg with the support posts. (The 15-deg angle was the maximum angle permitted by the existing test facility.) The results of three angle impact tests follow.

TEST E

The vehicle in this test was directed into inner support B at a speed of 28.6 mph. The 3,920-lb Ford activated the breakaway connections satisfactorily and the support cleared the vehicle adequately. The load distributors were deformed very slightly and the truss rotated only 1 deg. The results of this low-speed, 15-deg angle test were similar to those observed in head-on Test A conducted at nearly the same impact speed. Damage to the test car, shown in Figure 16, was produced by a decelerative unit force of 3.7 g; and the peak decelerations were observed on electronic records to be 8.8 g (longitudinal) and 3.4 g (transverse).

TEST F

This test was conducted because in an earlier test the compact vehicle snagged the breakaway support. The 2,350-lb Borgward used in this test is similar in appearance to the 2,100-lb Simca which was tested earlier. Vehicle speed was 52 mph. During the interaction between vehicle and support, a slight lifting of the vehicle was observed. The front of the vehicle was elevated approximately 8 in. off the ground, but the support then rotated

Figure 16. Vehicle after Test E.

Figure 17. Vehicle after Test F.

Figure 18. Damage to truss guide angle (Test F).

away from the vehicle, allowing it to clear the car. The average longitudinal deceleration was 12.2 g; the maximum observed longitudinal deceleration was 30.8 g, occurring at 0.041 second after impact, and the maximum transverse deceleration of 9 g occurred at about the same time. These deceleration levels, bordering on the unacceptable from a passenger tolerance point of view, illustrate the problem inherent in interactions with small vehicles (that is, interactions having a low ratio of vehicle-mass to support-mass). Vehicle damage is shown in Figure 17.

A new development in this test was the contact between the support and guide angles. Guide angles were installed in the truss, as shown in Figure 18, to prevent the support from striking vertical truss members during an angle hit. In this test, when the portion of the support above the hinge point contacted the guide angle, a chunk of steel, shown in Figure 19, was peeled from the toe of the angle, but there was no damage to the support. The damage to the guide angle had no effect on the structural integrity of the truss. However, some energy was absorbed by this action. The support deformed the load distributors on the lower truss chords significantly and twisted the truss through an angle of 4 deg. The upper connection bolts at support B were fractured. The support-post behavior in an angle impact with an outer support is shown in Figure 20, and the pendulum action of the support is clearly demonstrated as the post rotates about its pin connection first in the direction of the colliding vehicle, then past the lower base connection (t = 2.000 sec). As noted earlier, this swinging action continues for several seconds following impact with an outside support.

TEST G

A Ford weighing 3,950 lb collided with support A at 50.1 mph and an impact angle of 15 deg. The vehicle was slowed 10.2 mph as a result of the collision. The average decelerative unit force on the vehicle was 5.8 g, and the peak decelerations were observed to be 15.3 g (longitudinal) and 3.5 g (transverse). These peaks occurred at approximately 0.040 second after impact. Damage to the crash vehicle is shown in Figure 21.

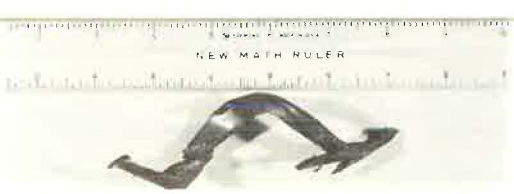

Figure 19. Splinter from guide angle.

The truss twisted through 8 deg and the upper connection bolts at support B were fractured. Upper connection bolts at sup-

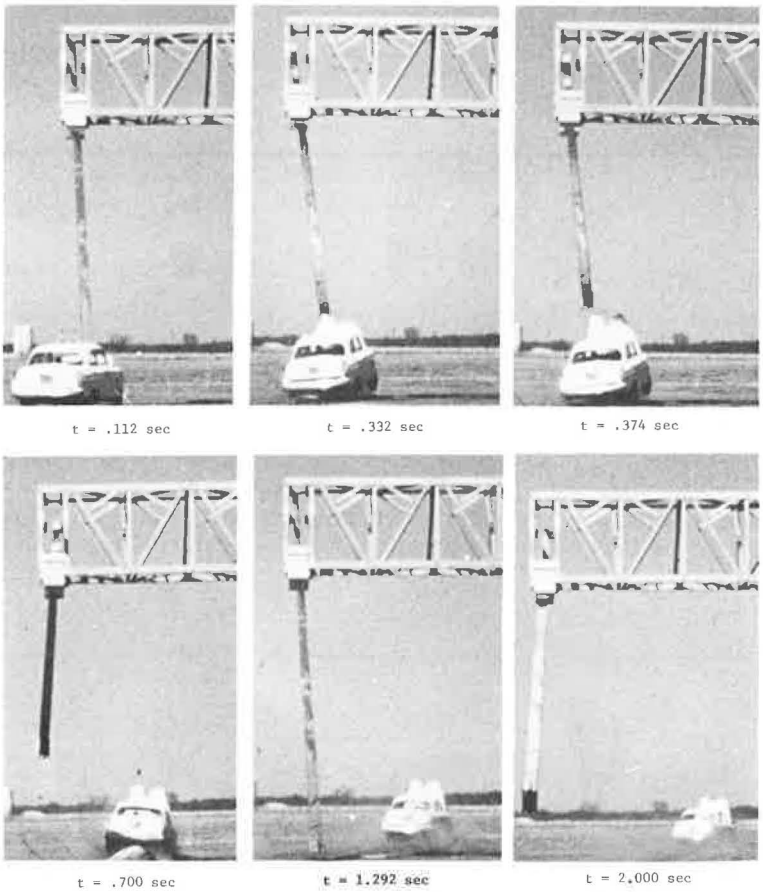

Figure 20. Sequential photographs of Test F.

ports C and D were removed, examined, and found to be undamaged. The structure remained erect and in good condition.

This test was conducted during a meeting of the Technical Subcommittee, at which two additional tests were proposed. Much discussion was devoted to the stability of the prototype structure when subjected to heavy vehicle loads at high impact speeds. At a later meeting of the Project Policy Committee it was decided to conduct two additional tests using heavy automobiles colliding with an outer and inner support.

Figure 21. Vehicle after Test G.

TEST H

Column A was struck head-on by a 5,150-lb Cadillac traveling at 75.3 mph. The upward rotating support ripped the hood from the car, continued upward, deformed the load distributors, and caused the truss to rotate about the pin connections. The upper connection bolts at columns B, C, and D fractured, and the truss continued to rotate until it came to rest in the position shown in Figure 22.

Figure 22. Condition of structure after Test H.

Figure 23. Crash vehicle after Test H.

The vehicle damage is shown in Figure 23. The average deceleration was 6.9 g and a peak of 17.6 g was observed on the accelerometer trace. The car was slowed 11.5 mph by the collision. The post penetrated the vehicle 2.08 ft. The entire structure remained upright following the collision, although the catwalk and lighting supports restricted clearance to approximately 12 ft.

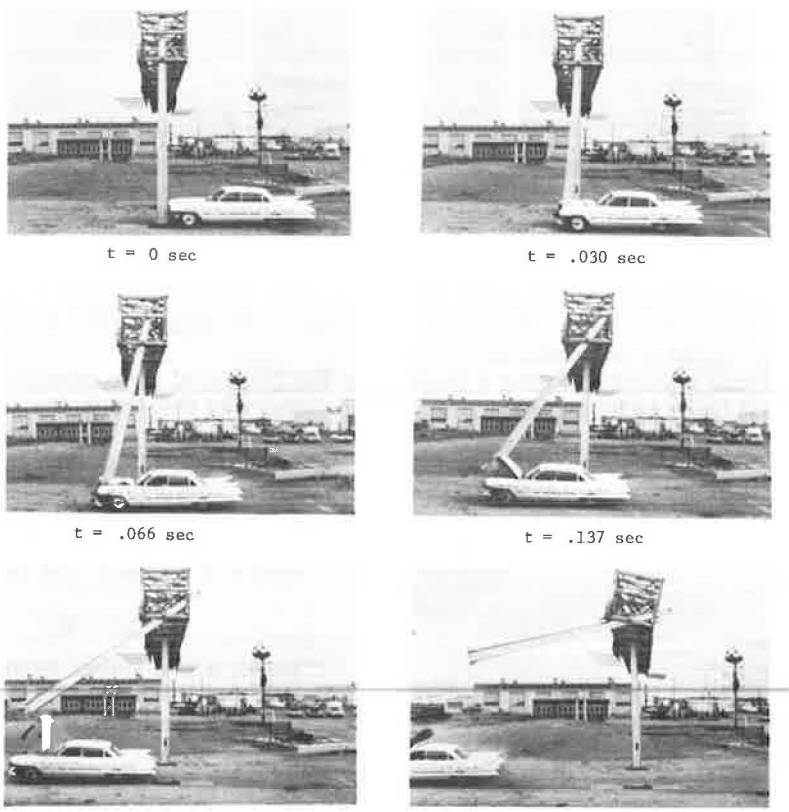

Figure 24. Sequential photographs of Test H.

Figure 25. Damaged vehicle after Test I.

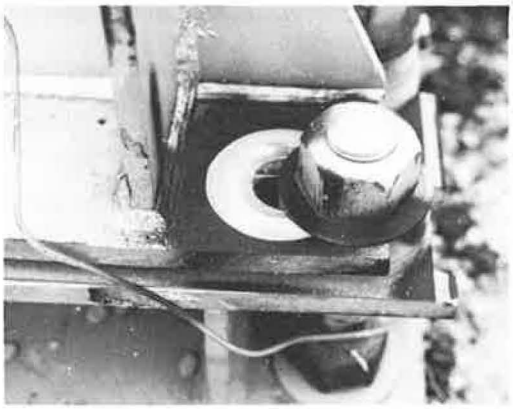

Figure 26. Breakaway base movement at column C (Test I).

TEST I

This final crash test was conducted on January 28, 1971. A 5,170-lb Cadillac struck column B at 72.0 mph and was slowed 11.2 mph by the impact. The sequence of events in the collision incident are shown in Figure 24, and damage to the car is shown in Figure 25. The average and peak decelerations are given in Table 1. The maximum post penetration was 2.6 ft.

Following the test, it was observed that the upper plate of the breakaway base at column C (Fig. 26) had slipped approximately 2 in. in the direction of vehicle impact. However, the truss and structure remained erect.

SUMMARY

At the outset this study was primarily concerned with the loads imposed by an automobile colliding with a breakaway overhead sign bridge support. Damage to the colliding vehicle, decelerative forces, and change in speed were of primary concern. As the study developed, it became clear that the behavior of the prototype truss and supports during a high-speed collision incident needed careful attention. Consequently, inside and outside supports were struck at angles of zero and 15 deg and load distributors and guide angles were developed and incorporated into the prototype structure.

CONCLUSIONS

1. The breakaway safety features of the overhead sign bridge reduce the collision forces on a standard-size vehicle to a level which is considered survivable for restrained passengers.
2. The prototype structure remained erect and suffered only localized damages during the series of tests reported.

ACKNOWLEDGMENTS

The research, development, and evaluation studies reported herein were sponsored by the highway departments of Alabama, Arkansas, Connecticut, Florida, Georgia, Hawaii, Kentucky, Louisiana, Maryland, Michigan, Mississippi, Montana, Nebraska, New Hampshire, New Mexico, Rhode Island, South Dakota, Tennessee, Texas, West Virginia, Wyoming, and the District of Columbia in cooperation with the Federal Highway Administration. Representatives from each of these agencies formed a Project Policy Committee which counseled the researchers during the course of this study. The Project Policy Committee appointed a Technical Subcommittee which provided guidance on structural and testing details.

At an early meeting, the deliberations of these engineers, administrators, and researchers led to a decision to conduct the testing program on the basis of increasingly severe conditions of impact, thus permitting interim evaluation of successive tests. As a result, damage to impacting vehicles and to parts of the prototype structure could be

observed and evaluated. Certain changes in the original design were necessary during the testing program.

The authors are deeply indebted to the members of the Project Policy Committee and the Technical Subcommittee and to the Contract Manager for their patience and counsel; furthermore, we thank them and their agencies for making this research effort possible.

REFERENCES

1. Martinez, J. E., Jumper, J. J., and Baskurt, F. Y. Mathematical Simulation and Correlation. Technical Memorandum 605-2, Texas Transportation Institute, Texas A&M University, Sept. 1970, pp. 24 and 25.
2. Ivey, D. L., Olson, R. M., Buth, C. E., and Hirsch, T. J. Testing Program. Technical Memorandum 605-4, Texas Transportation Institute, Texas A&M University, Sept. 1970.

WIND LOADS ON LOUVERED SIGNS

Hayes E. Ross, Jr., Texas Transportation Institute, College Station

Results of a series of wind tunnel tests of both straight and curved louver sign models are presented in this paper. A total of 16 different models were tested to determine the effect of louver angle, louver width, sign height to width ratio, and sign message on the wind loads. Dimensionless force and moment coefficients are presented in graphical form, providing a concise and convenient source of information for determining wind loads on full-scale louvered signs. Comparisons are made between the wind loads on a conventional sign and wind loads on louvered signs of various configurations. For a given frontal area, tests show that wind loads on a louvered sign are approximately 50 percent less than those on a conventional solid background sign. Gross estimates of louvered sign costs are given and compared with conventional sign costs. The visibility aspect of a louvered sign is briefly discussed. Actual field installations of louvered signs are shown and discussed.

•MANY signs on the Interstate freeway system are of necessity very large. Massive supports are required to resist the wind loads of these signs and as a consequence the supports present a hazard to motorists since the sign is usually in close proximity to the roadway. Economically, costs increase as the size of the sign's support structure increases.

Development of "breakaway" supports for roadside signs has greatly reduced the hazard. Research is now in progress on breakaway supports for overhead sign bridges.

Another concept which can reduce the hazard of the sign's supports and quite possibly the costs of the entire structure is the use of a louvered sign in lieu of the conventional solid-background sign. Tests have shown that the louvered sign can reduce wind loads on a conventional sign by 50 percent. Considerable reduction in the mass of the supports could be expected as a result of the reduced wind loads. Analysis of breakaway supports for sign bridges at the Texas Transportation Institute have shown that as the mass of the support is reduced impact forces on a colliding vehicle are reduced.

Recent studies of wind loads on solid-background conventional signs were conducted at TTI and have been documented (1). However, research in the area of nonsolid signs has been very limited. The only published data available on nonsolid sign backgrounds specifically is that of Tidwell and Samson (2). In their study, several types of nonsolid configurations were model tested, viz., expanded metals, honeycomb materials, and a louvered sign. Of the types tested, the louvered configuration appeared to offer the greatest promise from the standpoint of wind-load-reducing capabilities and visibility. When compared to a flat plate, the louvered model showed a 57 percent reduction in maximum force and an 83 percent reduction in twisting moment. It also provided a solid appearance.

A literature survey of topics within the aerodynamics field revealed that a very limited amount of information existed which could be applied to the investigation of wind loads on louvered signs. Previous work in the area of louvers (or cascaded airfoils)

Sponsored by Committee on Traffic Safety Barriers and Sign, Signal and Lighting Supports and presented at the 50th Annual Meeting.

has, for the most part, been directed toward turbine or axial compressor applications (3). In most of these cases, the cascades were smooth airfoil shapes and were oriented at small angles of attack (less than 10 deg), in which case the air flow over and under the cascade does not separate. For the flat plate cascades (as in the louvered sign) the air flow will separate for all but the smaller angles of attack (about 15 deg or less).

TEST PROCEDURE

Since the studies of Tidwell and Samson were limited to one particular louver configuration more information was needed on the relationship between wind loads and louver angle, louver width, and the sign height to width ratio. To determine these relationships 13 straight-louver sign models and 3 curved-louver models were constructed. Details of these models are shown in Figures 1 and 2.

To assemble the models the louvers were fillet welded to the side plates. The windbeams were then welded to the side plates, and the mounting gussets were bolted to the windbeams and welded to the support pole.

Models 1 through 3 were used to determine the effects of the wind-tunnel wall interference on the measured wind loads. For any given wind tunnel there is a limit to the model size that can be tested before appreciable errors occur in the measured wind loads. Models 3 through 11 were used to determine the amount by which the wind loads were affected by variations in the louver angle, louver width, and Reynolds number. Models 7, 12, and 13 were used to determine the wind load variations as a function of the model's height to width ratio, sometimes called the aspect ratio.

To compare the results, the tests were all conducted at a constant Reynolds number ($R_E = 1.56 \times 10^5$), with the exception of the Reynolds number tests. The louver width was chosen as the characteristic length in the Reynolds number.

In designing the curved louver models, advantage was taken of the flat-plate louver tests. Results from these tests showed that the wind loads were practically independent of lower width. For this reason only three models were needed in the curved

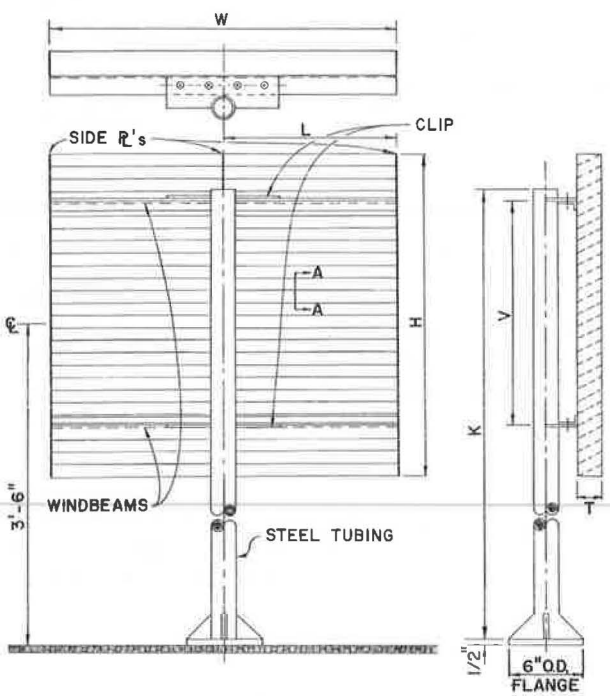

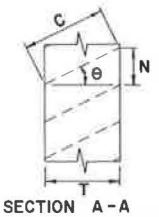

MODEL SCHEDULE

MOD NO.	LOUVER L	C	NO REQ'D	θ	N	SIDE ℄ H	T	MISC. W	K	V
1	21	2.8	42	45°	2	42.0	2	42.4	60.5	28
2	15	2.8	30	45°	2	30.0	2	30.4	54.5	20
3	12	2.8	24	45°	2	24.0	2	24.4	51.5	18
4	12	2	34	45°	1.4	23.8	1.4	24.4	51.5	18
5	12.1	2.3	30	45°	1.6	24.0	1.6	24.6	51.5	18
6	12	2	48	30°	1.0	24.0	1.7	24.4	51.5	18
7	11.9	2.3	44	30°	1.1	24.2	2.0	24.2	51.5	18
8	12	2.8	34	30°	1.4	23.8	2.4	24.4	51.5	18
9	11.9	2	92	15°	.52	23.9	2.0	24.2	51.5	18
10	12.1	2.3	82	15°	.59	24.2	2.2	24.6	51.5	18
11	12	2.8	66	15°	.73	24.1	2.7	24.4	51.5	18
12	15.5	2.3	28	30°	1.1	15.3	2.0	31.4	47.0	8.9
13	8.9	2.3	48	30°	1.1	27.0	2.0	18.2	53.0	21

Figure 1. Details of straight-louver sign models.

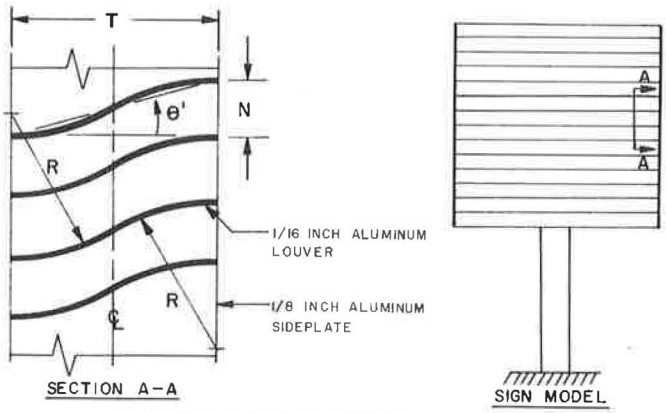

MODEL SCHEDULE

MOD. NO.	LOUVER L*	C**	R	θ'	N	NO. REQD	SIDE PLATE H*	T	MISC. W*	K*	V
14	24.0	4.60	2.50	26.6°	2.0	12	24.0	4.0	24.4	51.5	18.0
15	24.0	4.37	3.05	20.6°	1.5	16	24.0	4.0	24.4	51.5	18.0
16	24.0	4.17	4.26	14.1°	1.0	24	24.0	4.0	24.4	51.5	18.0

*REFER TO FIGURE 1 FOR GEOMETRIC DESCRIPTION
**ARC LENGTH

Figure 2. Details of curved-louver sign models.

louver tests. From these three models the relation between wind load and louver angle could be ascertained.

The models were tested in the 7- by 10-ft Low Speed Wind Tunnel at Texas A&M University. Figure 3 shows a front and rear view of model number 5 in the wind tunnel. Sign model number 8 was tested with and without a typical message. Model 8 with the message attached is shown in Figure 4. Curved louver model number 14 is shown in Figure 5.

All the models were subjected to wind velocities in the 0 to 100-mph range.

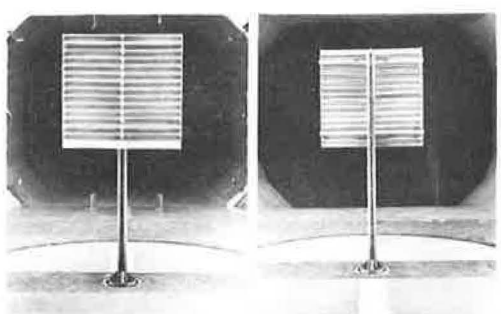

(a) FRONT VIEW (b) REAR VIEW

Figure 3. Louvered model no. 5 mounted in wind tunnel.

(a) NORMAL VIEW (b) SIDE VIEW

Figure 4. Louvered model no. 8 with message.

TEST RESULTS

For convenience, results of the wind tunnel tests were reduced to dimensionless coefficient form. These coefficients are defined as follows:

$$C_N = \frac{F_N}{qA_S} = \text{normal-force coefficient;}$$

$$C_T = \frac{F_T}{qA_S} = \text{side-force coefficient;}$$

$$C_L = \frac{F_L}{qA_S} = \text{lift-force coefficient; and}$$

$$C_{MT} = \frac{M_T}{qA_S W} = \text{twisting-moment coefficient,}$$

where

F_N = total normal force;
F_T = total side force;
F_L = total lift force; and
M_T = total twisting moment.

} These actions are shown in Figure 6 in their positive directions.

Also,

A_S = frontal area of sign;
q = impact pressure = $\frac{1}{2} PV^2$;
P = mass density of air;
V = velocity of air; and
W = width of sign.

Reynolds R_N number is defined by

$$R_N = \frac{Vl}{\nu}$$

where

l = width of louver, and
ν = kinematic viscosity of air.

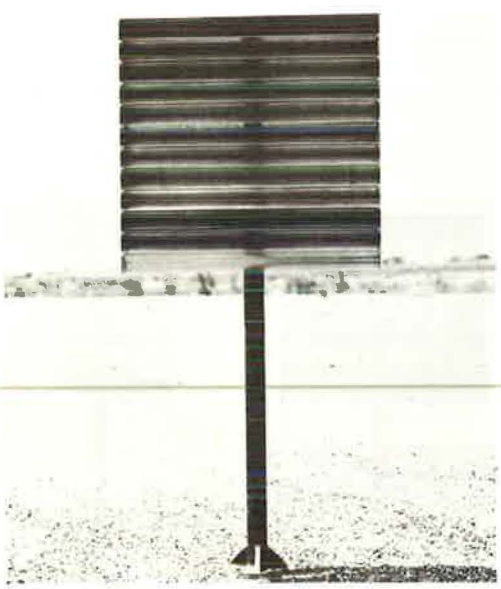

Figure 5. Curved-louver model no. 14.

Necessary limitations on the size of this paper prohibit a full presentation of all test results. Nevertheless, the major findings of the study are presented in the following sections. Full details of the study have been reported elsewhere (4).

Straight Louver Tests

Curves of the normal-force coefficient, side-force coefficient, lift-force coefficient, and twisting-moment coefficient are shown in Figures 7 through 10, plotted against the angle of attack α (Fig. 6). Each figure shows the results of the three louver-angle configurations for the 2.8-in. louver width. The other curve in Figures 7 and 10 is the result of a flat-plate model test and is included for comparative purposes. Similar results were obtained for the 2.0-in. and 2.3-in. louver widths.

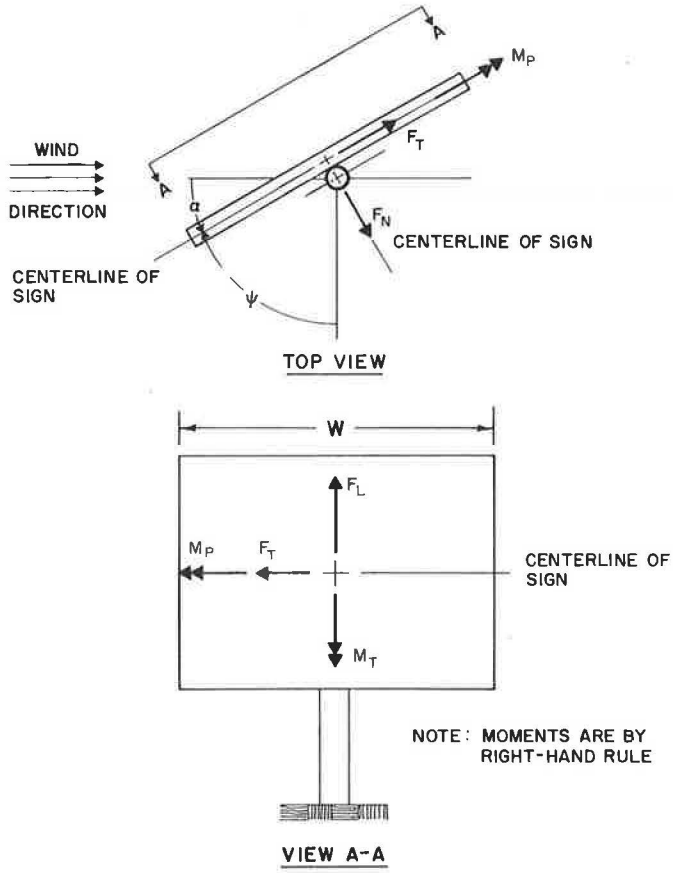

Figure 6. Positive sign convention for sign axis system.

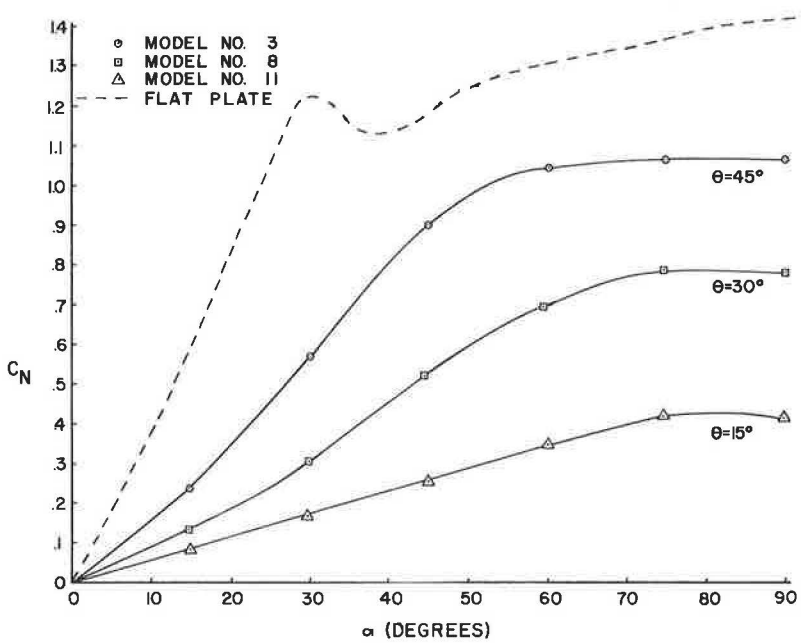

Figure 7. Normal-force coefficient versus angle of attack for straight-louver models, louver width = 2.8 in.

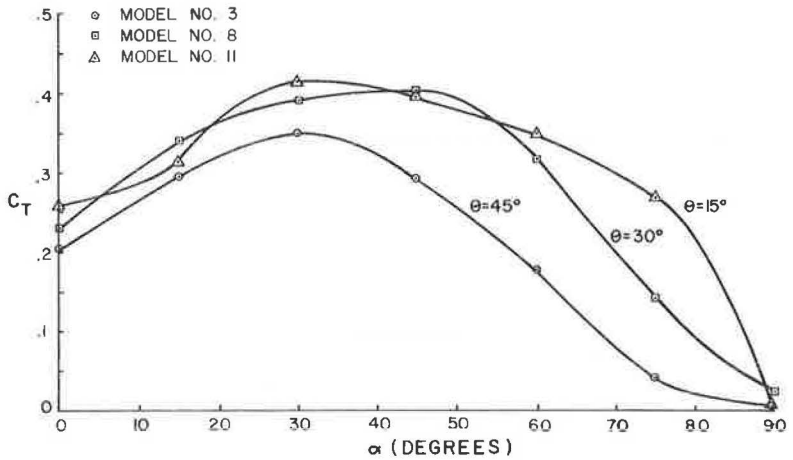

Figure 8. Side-force coefficient versus angle of attack for straight-louver models, louver width = 2.8 in.

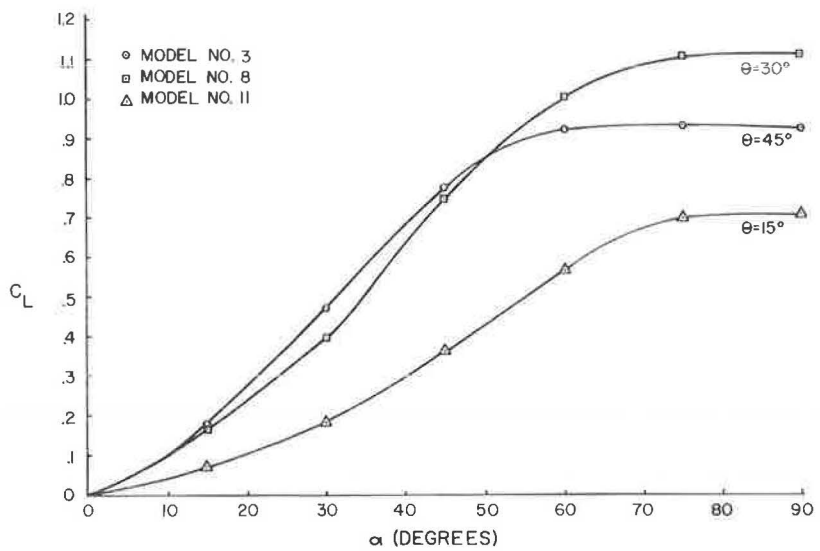

Figure 9. Lift-force coefficient versus angle of attack for straight-louver models, louver width = 2.8 in.

Variations in the normal-force coefficient with louver angle are shown in Figure 11 for the three louver widths. The comparison is shown at an angle of attack of 90 deg. In most cases this is the angle at which the coefficient obtained its maximum value.

It is noted that the variations in the normal-force coefficient are not necessarily attributable to the difference in louver angles alone. The distance between the louvers is dependent on the louver angle and the spacing is therefore different for any two louver angles. Hence, the variations in the coefficients may include the effect of the different louver spacings also.

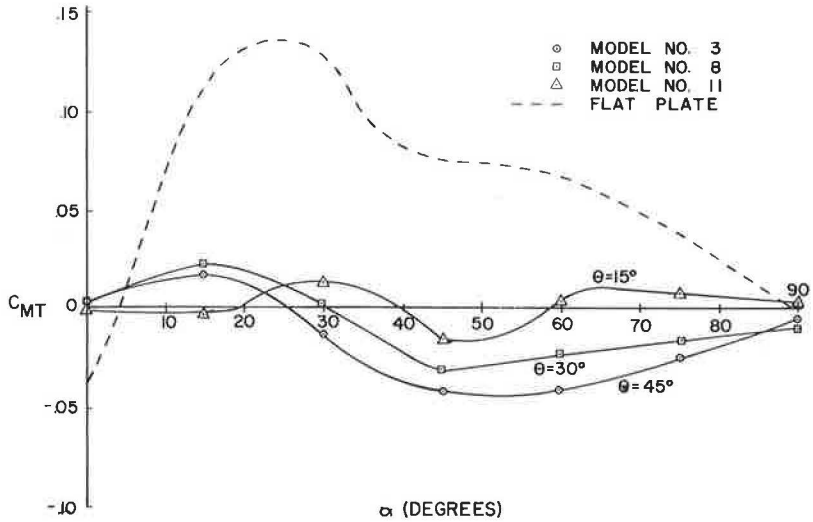

Figure 10. Twisting-moment coefficient versus angle of attack for straight-louver models, louver width = 2.8 in.

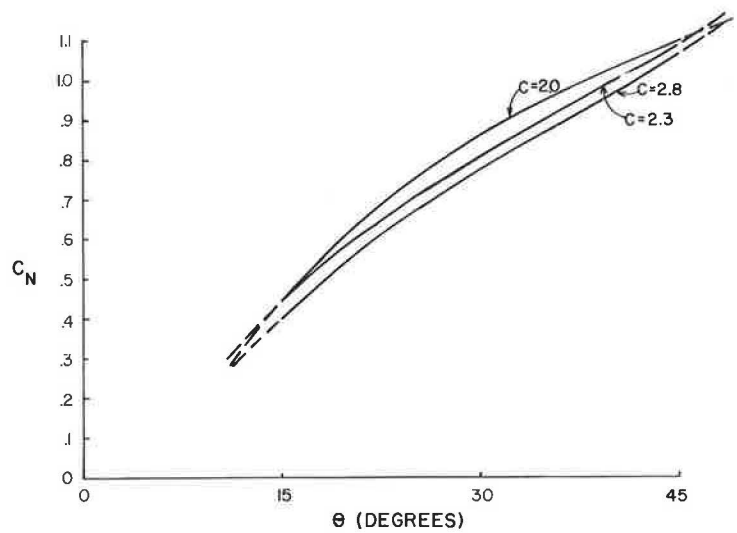

Figure 11. Normal-force coefficient versus louver angle for straight-louver models at α = 90 deg.

The louver spacing on each model was such that a solid appearance was maintained without any louver overlap. As a result, the louver spacing was different on models 3 through 11. An overlap is not necessarily detrimental from either an aerodynamic standpoint or a visibility standpoint. The decision not to overlap was based on economic considerations. It seemed apparent that the cost would increase as the louver overlap increased.

The four coefficient values were found to be practically independent of the aspect ratio and Reynolds number. The normal-force coefficient, twisting-moment coefficient,

and the lift-force coefficient were found to be independent of louver width. As expected the side-force coefficient increased as the louver width increased (the width of the side plate increases as the louver width increases).

Model number 8 was equipped with a typical message in order to determine message effects on the wind loads. Although the message caused an increase in the normal force by about 12 percent, it reduced the side- and lift-forces by approximately 10 and 30 percent respectively. Although only one model was tested for message effects, the information obtained is considered to be applicable to the other configurations.

No extreme flutter problems were encountered during the straight louver test. The longest unsupported louver length was 15.5 in. on model number 12. The top and bottom louvers of all models experienced varying degrees of flutter, depending upon the louver configuration, sign angles of attack, and wind velocity. In general, the flutter was more pronounced in the models with the larger louver angles, at a sign angle of attack of 90 deg, and for wind velocities from 80 to 100 mph. The flutter did not become catastrophic in any case and is not believed to be a serious problem. A plate over the top and bottom louvers, making in effect a box-frame for the sign, would likely eliminate the flutter, at the expense of a slight increase in the normal wind force.

Curved Louver Tests

Figure 12 shows the normal-force coefficient versus the angle of attack for the three curved louver models. The maximum values of the coefficient, 0.53 at $\theta' = 26.6$ deg, 0.4 at $\theta' = 20.6$ deg, and 0.31 at $\theta' = 14.1$ deg, are considerably less than the corresponding flat-plate value of 1.4 (Fig. 7).

The side-force coefficients were slightly higher than the straight louvered values. The larger values are attributed in part to the wider side plates used in the curved louver models. Also, the nature of the air flow through the curved louver models likely contributed to the side-force differences.

The geometry of the curved louvers causes a momentum change in the air flow which acts to produce a pitching moment (M_P in Fig. 6) on the background. The pitching moment must be added to that caused by the normal force.

The curved-louver coefficients were found to be independent of Reynolds number. The characteristic length chosen for the Reynolds number was the distance between the

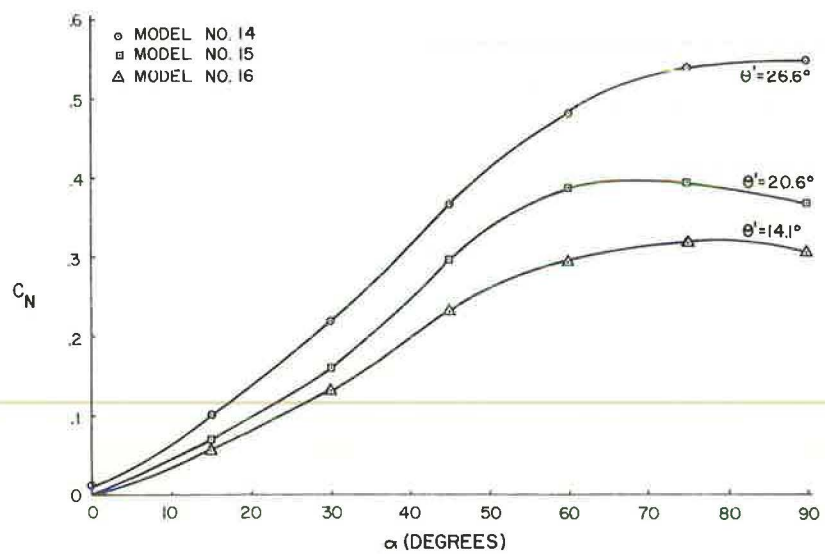

Figure 12. Normal-force coefficient versus angle of attack for curved louvers, side-plate width = 4.0 in.

forward and rear edge of the curved louver. It is the hypotenuse of the triangle whose sides are the side-plate width and the louver spacing.

No data are available on the variations in the coefficients as the aspect ratio is varied for curved louvers, since the three models tested all had the same aspect ratio (1.0). However, it is unlikely that appreciable variations would exist, at least within the range of aspect ratios of most highway signs, since the variations were negligible in the straight-louvered models.

The curved louvers experienced a greater degree of flutter than the straight louvers. The flutter was evident at a wind speed of approximately 75 mph and increased in intensity as the wind speed increased. As in the straight louvers, the flutter was much more pronounced in the upper and lower louvers. The corrective action recommended in the straight-louver flutter problem should also reduce the curved-louver flutter problem.

All of the louver model coefficients include the effects of the windbeams and that part of the supporting pole directly behind the model. The frontal area of the windbeams blocking the air flow totaled about 0.25 sq ft. This comprised about 6.3 percent of the sign's frontal area. The total blockage by windbeams on full-scale signs would likely be about the same amount. Hence, the coefficients can be used in most cases without alterations due to windbeam effects.

It is not recommended that the coefficients be used to include the effects of the sign supports, although the coefficients included the effects of a portion of the model support. The single tubular support is not believed to have affected the wind loads on the models to any extent. In actual design, the wind loads on the sign supports should be computed separately and then added to the background wind loads.

All of the coefficients are shown for positive angles of attack, i.e., wind impinging on the front of the sign. However, the models were tested at negative angles of attack also. The results with negative angles were similar to those at positive angles, with one exception. Winds on the back side of the model caused a negative lift. In designing the sign supports the negative lift would likely be more critical, since it would be a compressive load.

CONVENTIONAL SIGNS VERSUS LOUVERED SIGNS

Wind Loads

A comparison was made between the wind loads that would exist on a straight-louver and a curved-louver sign and a geometrically similar conventional sign. The straight-louver values are based on a lower width of 2.8 in. In the straight-louver case, the wind loads include the effects of a typical message on the sign. A sign having 100 sq ft in frontal area with an aspect ratio equal to 1.0 was chosen as a typical example. The comparative summary is given in Tables 1 and 2.

TABLE 1

STRAIGHT-LOUVER MODEL RESULTS, LOUVER WIDTH = 2.8 IN.

Wind-Load Force Component	Louver Angle (θ)			Flat Plate
	15 deg	30 deg	45 deg	
Maximum normal force F_N (lb)	1,288	2,109	2,867	3,841
Reduction in flat-plate normal force (percent)	66	45	25.4	—
Maximum side force F_T (lb)	1,039	845	707	256
Increase in flat-plate side force (percent)	306	230	176	—
Maximum lift force F_L (lb)	818	1,993	1,507	0
Weight of sign (lb)	450	290	210	300
Decrease (increase) in flat-plate weight (percent)	(50)	3.3	30	—

TABLE 2

CURVED-LOUVER MODEL RESULTS

Wind-Load Force Component	Louver Angle (θ')			Flat Plate
	14.1 deg	20.6 deg	26.6 deg	
Maximum normal force F_N (lb)	1,067	1,259	1,654	3,841
Reduction in flat-plate normal force (percent)	72	67	57	—
Maximum side force F_T (lb)	960	975	991	256
Increase in flat-plate side force (percent)	275	281	287	—
Maximum lift force F_L (lb)	358	851	1,609	0
Weight of sign (lb)	500	370	320	300
Increase in flat-plate weight (percent)	67	23	7	—

An additional force component must be considered in the louvered sign when compared to the conventional sign. That component is the lift force, which acts in either the upward or downward direction, depending upon the wind direction. However, its effect on the structural designs of the sign would probably be small.

The sign weights are based on an aluminum-louvered sign and a plywood conventional sign. The weights include the windbeams but exclude the sign supports.

Costs

Evaluating the economic aspects of the louvered sign proved to be a difficult task. Cost estimates obtained from different industrial firms varied. After considering the estimates it appears that the cost of a straight-louvered aluminum background would be roughly as follows:

Louver Angle	Cost per Sq Ft
15 deg	$5.00 to $6.00
30 deg	$4.50 to $5.50
45 deg	$4.00 to $5.00

These values include the material and fabrication cost of the background but exclude the material and attachment cost of the windbeams, supports, and message. The geometry of the background, for which these prices are based, was similar to that of the models, i.e., a series of 0.0625-in.-thick louvers, 12 in. in length, interlocked by vertical plates (sideplates).

No prices are available on the cost of material other than aluminum. Curved-louver background costs are also unavailable. However, it is likely that their cost would be comparable to the straight louver, using the louver angle (θ) in the straight louvers and the effective louver angle (θ') in the curved louvers as a basis for comparison. The curved louver could probably be extruded for a cost not greatly exceeding the straight louver. The wider unsupported lengths allowable in the stiffer curved louvers would tend to offset the cost differences between the two configurations.

The cost of a plywood background for the conventional signs is estimated to be 75 cents per sq ft. This price would include the cost of the plywood, splice plates, fasteners, and labor to assemble. All other costs are excluded. This price can then be compared with the previously quoted prices for louvered sign backgrounds.

Visibility

The ability of both the curved and straight louvered models to display a message appeared adequate. With the background of the model painted green, the white painted message was clearly visible from the usual viewing angles. Refer to Figure 4 for two views of a straight-louvered model (louver angle = 30 deg) with a message attached.

IMPLEMENTATION

Shown in Figures 13 and 14 are two full-scale louvered signs that have been installed on an experimental basis in the state of Illinois. In Figure 13 the sign on the right is

Figure 13. Conventional and louvered sign on overhead sign bridge.

Figure 14. Shoulder-mounted louvered sign.

louvered and the one on the left is a conventional solid-background sign. The appearance of the message on the louvered signs seems as legible as that on the conventional sign.

The signs shown in Figures 13 and 14 contain curved louvers very similar in geometry to those described in this paper. The louver angle (θ') is approximately 30 deg and the louver width is approximately 3.6 in. Preliminary analysis indicates that wind-load reductions of about 50 percent are being experienced through the use of these louvered signs. Further studies are planned at Illinois with these experimental signs to determine if snow accumulates in the louvers and to determine the cost effectiveness of the sign and its support structure.

CONCLUSIONS

Tests have shown that reductions of approximately 50 percent in wind loads can be realized by the use of louvered signs in lieu of conventional flat-plate signs. Such a reduction would allow a considerable reduction in the weight of the sign's support members, thereby reducing the hazard the sign presents to motorists and the cost of the support structure.

Preliminary observations indicate that the louvered sign can display a message adequately.

It is apparent that the louvered sign itself will be more expensive than a conventional flat-plate sign. Cost-effective studies are needed, however, to determine if reductions in support costs and accident costs would compensate for the increased sign cost. In the author's opinion the study would show that an overall reduction in cost could be realized if louvered signs were employed in lieu of conventional signs, especially in the large overhead sign bridges.

Although models were used to obtain wind loads, tests showed that the dimensionless force and moment coefficients were independent of sign size and shape. The data presented thus provide a concise and convenient source of information for determining wind loads on full-scale louvered signs.

ACKNOWLEDGMENTS

Information in this paper was developed at the Texas Transportation Institute as part of a multistates' cooperative research endeavor financed under the Highway Planning and Research Program by a contract with the Federal Highway Administration, Department of Transportation. The research was made possible through the cooperative highway department participation of: Alabama, California, Illinois, Kansas, Louisiana, Minnesota, Mississippi, Nebraska, North Dakota, Oklahoma, South Dakota, Tennessee, Texas, and the District of Columbia. The author also thanks Mr. W. A. Frick of the Division of Highways of Illinois who furnished photographs and information concerning their experimental work on louvered signs.

The opinions, findings, and conclusions expressed in this publication are those of the author and not necessarily those of the Federal Highway Administration and/or those of the state highway departments.

REFERENCES

1. Ross, H. E., Jr., Olson, R. M., and Gaddis, A. M. An Investigation of Wind Loads on Roadside Signs. Highway Research Record 222, 1968, pp. 1-11.
2. Tidwell, D. R., and Samson, C. H. Wind Tunnel Investigation of Non-Solid Sign Backgrounds. Highway Research Record 103, 1965, pp. 1-9.
3. Harlock, J. H. Axial Flow Compressors. Butterworth Scientific Publications, London, 1958.
4. Wind Loads on Roadside Signs. Volume 2 of Final Report of Project HPR-2(104), Highway Sign Support Research, Texas Transportation Institute, College Station, 222 pp., July 1967.

IMPACT-YIELDING SIGN SUPPORTS

John P. Cook and Andrew Bodocsi, University of Cincinnati

This paper presents the results of an investigation of the steel-channel sign supports currently used by Ohio and many other states. These steel supports when struck by an automobile were found to yield at the ground line, and the impacting vehicles showed deceleration values well within human tolerance levels. The study included a laboratory simulation of the crash tests, a computer program to extrapolate the results, and a full-scale field testing program. The field testing program included 40 crash tests with velocity, sign type, angle-of-collision incidence, and soil-support conditions as the variables.

•A GREAT deal of research has been conducted on breakaway sign supports (1, 2). Biomedical research has also been conducted to determine the effects of deceleration impact on the human body (3, 4, 5, 6).

Breakaway sign supports have been shown to be effective in reducing injury when very large double-posted signs are used. However, the steel-channel supports used for small and intermediate-size signs had never been investigated. This study was conducted to determine the properties of these smaller size posts. In this work, signs of up to 56 sq ft of sign area were considered.

The breakaway sign support, upon impact, shears off at the base and the post swings up and out of the path of the vehicle. On the other hand the yielding sign support yields at the ground line and swings downward. The vehicle then passes over the post.

OBJECTIVES OF THE STUDY

A study of pictures and accident reports indicated that the steel-channel sign supports currently in use by the State of Ohio yielded on impact, with minimum damage to car and occupants. The objective of this study, therefore, was to determine definitively whether the channel posts are actually yielding sign supports and to provide, where necessary, criteria for redesign for maximum safety.

The steel-channel posts are provided in sections weighing 2, 3, and 4 lb per ft. The 3- and 4-lb sections are bolted back to back to form sections of 6 and 8 lb respectively. Figure 1 shows a typical channel post section. Figure 2 shows the sections bolted back to back to form a "piggyback" or "X" configuration.

Variables considered in the program were: post size, type, and material; sign-marker size and shape; support conditions; vehicle weight; vehicle velocity; angle-of-collision incidence; and sign type (single or double posted).

DESCRIPTION OF THE RESEARCH

The research program was divided into four phases:

1. Preliminary field testing to determine the range of the variables involved;
2. Laboratory testing on a crash simulator;
3. Computer programming to simulate and extrapolate the results; and
4. Field testing to verify the laboratory and computer work.

Sponsored by Committee on Traffic Safety Barriers and Sign, Signal and Lighting Supports and presented at the 50th Annual Meeting.

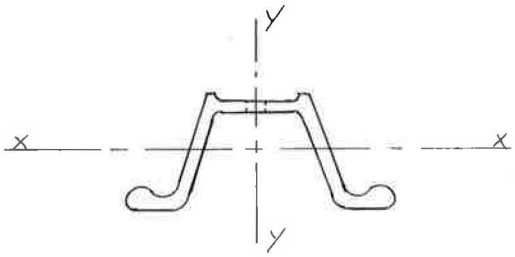

Figure 1. Typical channel section.

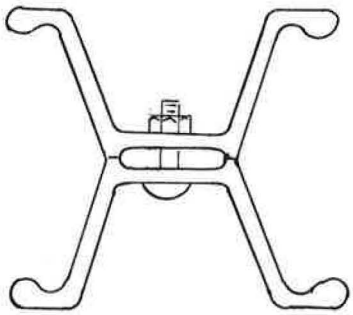

Figure 2. Typical piggyback section.

Preliminary Field Testing

The preliminary field testing consisted of six tests on posts of various sizes. These tests were monitored only by high-speed photography. The purposes of the series were to determine whether the steel post did actually yield under impact and to determine the damage to the impacting vehicle and the amount of deceleration.

The following information was obtained from the preliminary test series. Those tests are identified as 1817-1 through 1817-6 in Table 1.

TABLE 1

RESULTS OF FIELD CRASH TESTS

Test No.	Sign Type	Velocity (mph)	Incidence	Peak g	Average
1817-1	3-lb single	45	Head on	1.18	0.2
1817-2	4-lb single	45	Head on	4.26	1.33
1817-3	6-lb single	45	Head on	5.84	2.50
1817-4	8-lb single	45	Head on	5.12	1.86
1817-5	3-lb double	45	Head on	Est. 1.0	Poor film
1817-6	6-lb double	45	Head on	6.60	2.78
1817-7	2-lb single	10	Head on	Not recorded	
1817-8	2-lb single	20	Head on	Not recorded	
1817-9	2-lb single	30	Head on	Not recorded	
1817-10	2-lb single	40	Head on	Not recorded	
1817-11	3-lb single	10	Head on	1.66	0.30
1817-12	3-lb single	20	Head on	0.91	0.08
1817-13	3-lb single	30	Head on	3.45	1.15
1817-14	3-lb single	40	Head on	6.22	3.42
1817-15	3-lb single	10	45 deg	0.84	0.11
1817-16	3-lb single	20	45 deg	2.10	0.50
1817-17	3-lb single	30	45 deg	2.66	0.74
1817-18	3-lb single	40	45 deg	3.20	1.0
1817-19	4-lb single	10	Head on	0.54	0.08
1817-20	4-lb single	20	Head on	2.11	0.60
1817-21	4-lb single	30	Head on	1.86	0.53
1817-22	4-lb single	40	Head on	2.90	1.18
1817-23	8-lb single[a]	45	Head on	9.28	2.25
1817-24	6-lb single	30	Head on	2.54	0.59
1817-25	8-lb single	45	Head on	8.76	3.11
1817-26	6-lb double	30	Head on	4.12	1.64
1817-27	8-lb double	30	Head on	5.88	1.73
1817-28	6-lb double	30	Head on	7.56	2.71
1817-29	8-lb single	30	Head on	7.40	2.60
1817-30	8-lb double	45	Head on	8.86	3.10
1817-31	8-lb single[a]	50	Head on	6.50	1.16
1817-32	6-lb single[a]	50	Head on	4.12	1.18
1817-33	4-lb single	30	45 deg	3.06	0.74
1817-34	6-lb double	45	45 deg	5.65	Not reported
1817-35	6-lb single[a]	45	45 deg	7.15	2.1
1817-36	8-lb double	30	45 deg	3.88	0.97
1817-37	8-lb double	45	Head on	4.02	1.73
1817-38	6-lb double	45	Head on	3.96	1.64
1817-39	6-lb single	30	45 deg	4.20	1.06
1817-40	8-lb double[a]	40	Head on	8.40	2.28

[a]Concrete embedment.

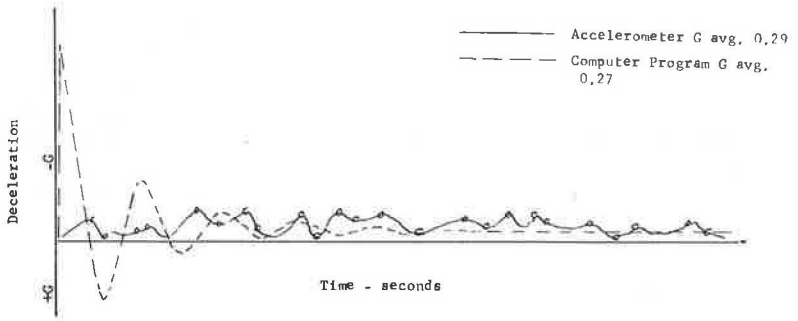

Figure 3. Laboratory test sand embedment.

1. The steel posts were found to be yielding posts when struck head-on at high velocity.
2. Deceleration values were found to be of a magnitude which could be measured by strain-gage accelerometers. The deceleration values were well within human tolerance levels.
3. Damage to the impacting vehicle was not serious. Only one test vehicle was used for all six preliminary tests.

Laboratory Testing Program

Research agencies throughout the country have used various types of simulators for studying impact behavior. The pendulum is the most widely used device, but hydraulic sleds have also been used.

The simulator used in this project was simply a scaled-down field test. The impacting vehicle was a small Fiat and the posts were usually the two-pound sections. The posts were set in a replaceable soil box and the compaction of the soil was carefully controlled.

The impacting vehicle was powered by a falling weight. The weight was a 1½-ton roller from a nearby steel mill, hoisted by winch to the top of the tower. As the weight was raised, the Fiat was pulled backward by a system of cables and pulleys until reaching the rear end of its track, when a hook on the back bumper tripped automatically, which released the mill weight sending the Fiat forward into the sign support. At the completion of each test, the complete soil box, including the deformed post, was lifted out of its pit and a fresh soil box hoisted into position. Spare soil boxes permitted the preparation of one post installation while another test was in progress.

Data collection in the laboratory simulation was exactly the same as for the full-scale field tests. Each test was recorded on high-speed film and recordings were taken from accelerometers mounted in the test vehicle.

Figure 3 shows the correlation between the laboratory tests and the computer simulation.

Computer Simulation

The computer program to describe the collision is basically a force, mass, acceleration equation. The post, the sign marker, and the supporting medium are idealized as shown in Figure 4. The complete system is then handled by the finite-element method, coupled with a step-by-step integration procedure. The precision of the results obtained is, of course, a function of the degree of precision of the input data. Apart from the specific terms in the equation itself, the number of time steps used becomes the prime factor in determining the precision of the results.

The basic matrix equation for the simulation is

$$\{P\}_t = [M] \cdot \{\ddot{\delta}\}_t + [C] \cdot \{\dot{\delta}\}_t + [K] \cdot \{\delta\}_t$$

where

$\{P\}_t$ = a vector of forces applied at the node points. Their value must be found by solving the dynamic interaction between the vehicle and the sign post.

$[M]$ = the mass matrix. The mass of the system is idealized as small masses lumped at the discrete node points. In a planar situation, there are displacement components in both the X and Y directions, and consequently the size of the mass matrix is twice the number of discrete node points in the system.

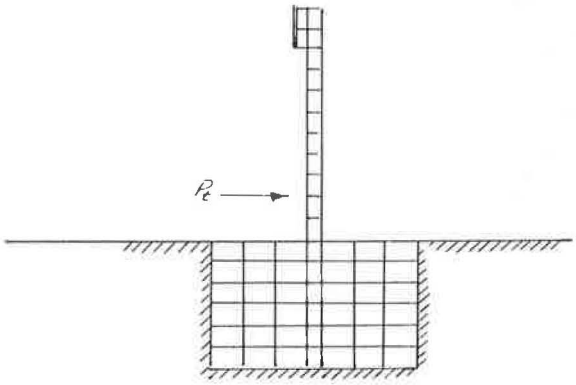

Figure 4. Idealized post.

$\{\ddot{\delta}\}_t$ = the accelerator vector. In simple terms this acceleration is the answer being sought. The acceleration varies with the time and furnishes a curve that yields both peak and average values of deceleration.

$[C]$ = the damping matrix. It is assumed to be proportional to the mass stiffness matrices in the following form: $[C] = \alpha \cdot M + \beta \cdot K$ in which α and β are constants related to the internal damping capacity of the system.

$\{\dot{\delta}\}_t$ = the velocity vector, which of course varies with time as the vehicle passes over the sign support.

$[K]$ = the stiffness matrix of the system. This matrix is formed in the same manner as the mass matrix, except that the individual stiffnesses, rather than the masses of the finite elements, are considered. The stiffness matrix is, of course, the same size as the mass matrix.

$\{\delta\}_t$ = the displacement vector. This vector also varies with time and furnishes the deflected shape of the sign support during the impacting time interval.

To obtain a suitable degree of precision, the system must be broken up into small elements, which of course increases the number of degrees of freedom of the system. Depending on the number of elements used, the program may involve 120 x 120 matrices, so that computer storage capacity becomes a serious problem.

A basic assumption of the program is that the problem is adequately represented by a two-dimensional system. This assumption was seriously questioned, since the angle-of-collision incidence is an important parameter of the problem. However, the full-size crash tests conclusively proved that the yielding sign posts, even when struck at a severe angle of incidence, twist into the plane of the impacting vehicle and yield as designed. Consequently the investigators feel that the assumption of the two-dimensional analysis is reasonably justified.

Figures 5 and 6 show the correlation between the computer simulation and the full-scale field tests.

Full-Scale Field Testing Program

The field testing program was conducted on a "drag strip" that was leased for this program. The strip was ¾ mile long and 30 ft wide so that several testing sites could be prepared simultaneously.

The crash vehicles in this program were towed up to speed and released. The crash vehicles were all standard-size automobiles. The towing vehicle was a ¾-ton Chevrolet pick-up truck. A 10-ft-long boom, made of 4 x 4 spruce, offset the crash vehicle from the tow truck as shown in Figure 7. The boom was pivoted at the center of the back bumper of the towing vehicle. Two tow ropes reached from the end of the boom

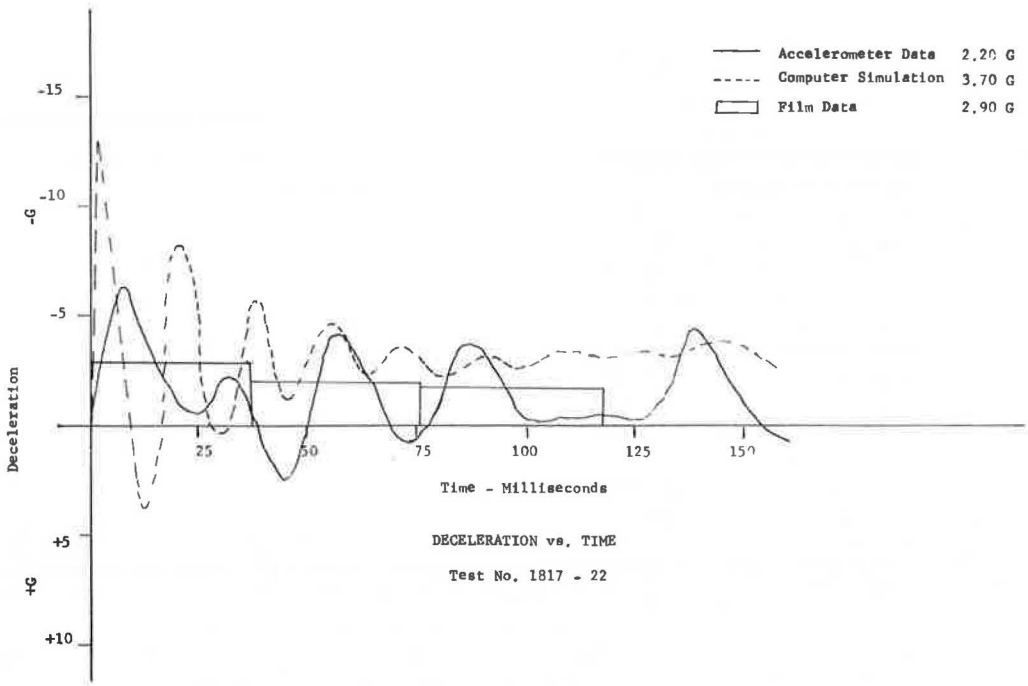

Figure 5. Deceleration versus time. Test no. 1817-22.

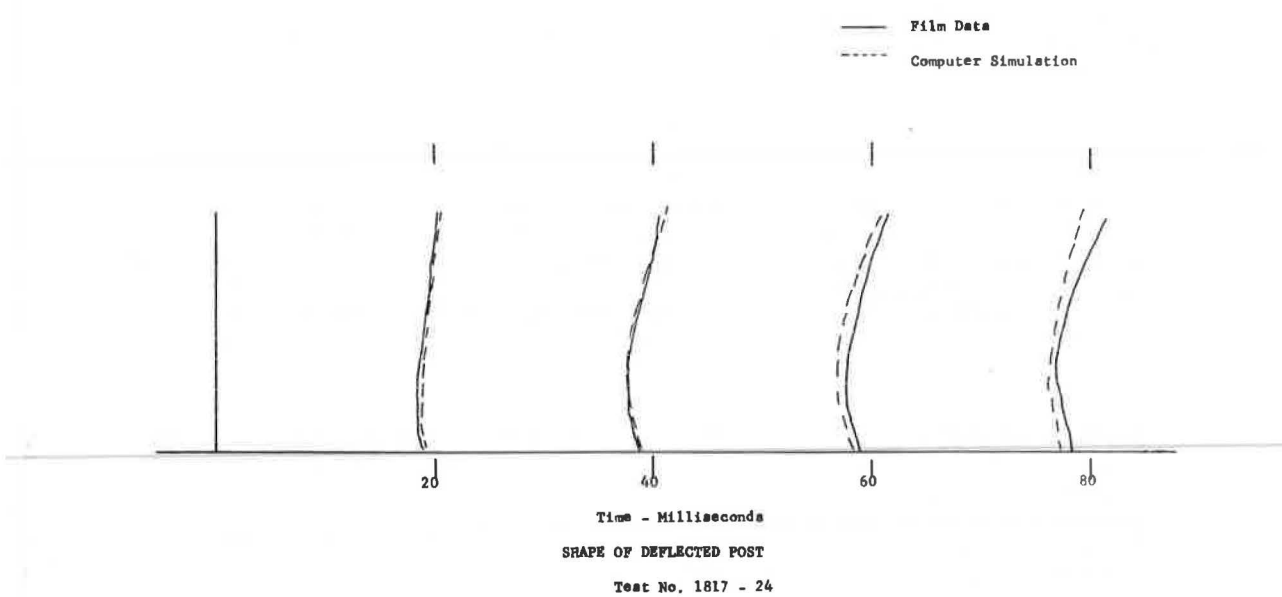

Figure 6. Shape of deflected post. Test no. 1817-24.

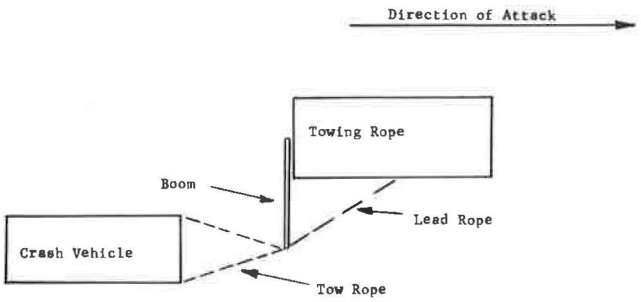

Figure 7. Towing apparatus.

to the crash vehicle. One lead rope attached the end of the boom to a release hook fastened to the frame of the truck. A solenoid controlled by a push button in the cab of the truck activated the release hook. No steering device of any kind was used in the crash vehicle. A steering control was designed and built, but never used, and the crash vehicle was controlled only by the driver of the towing vehicle.

Data Collection

Two systems of measuring deceleration were used. High-speed films were taken of each test and accelerometers were mounted in the test vehicle. Every test was photographed with a high-speed electrically operated camera. This camera operates at approximately 1,000 frames per second (compared to 64 frames per second for the ordinary movie camera). The camera was mounted 60 ft back from the test area on a 6-ft-high wooden platform. Photographic markers were mounted at 10-ft intervals along the edge of the test area, as shown in Figure 8.

At the completion of each series of tests the films were developed and still pictures were made of every 100th frame. This gave a permanent record of the position of the vehicle and the shape of the deflected post at $\frac{1}{10}$-second intervals. A manually operated film viewer permitted stopping the film at each frame for determining values of deceleration. Assuming a camera speed of 1,000 frames per second each frame of the film then represents one millisecond of elapsed time. Consequently a curve of deceleration versus time could be plotted from the deceleration data obtained from the film record.

The data collection system consisted of two accelerometers mounted in the crash vehicle. Various methods of mounting the accelerometers were considered. Mounting the accelerometers on the frame is probably the most stable arrangement, but the

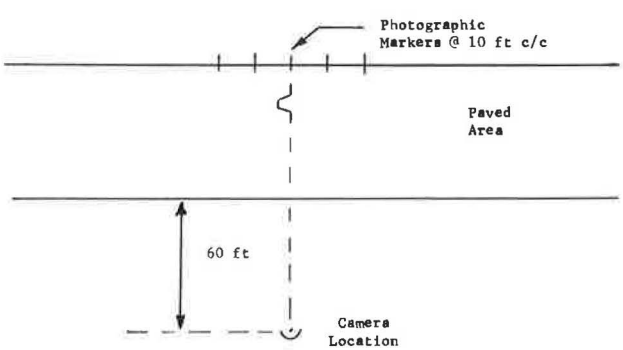

Figure 8. Plot plan showing camera location.

investigators felt that mounting the accelerometers directly in the passenger compartment would record values more representative of the actual shock experienced by the driver. Consequently the two accelerometers, one longitudinal and one transverse, were mounted on either the dash or the floor board of the passenger compartment.

An electronic signal from the accelerometers was picked up and stored on magnetic tape. The tape recorder was powered by an automobile battery and a DC to AC converter. The tape recorder, converter, battery, and a signal amplifier all rode in the crash vehicle. After each series of tests, the tape recorder was played back in the laboratory through a light beam oscillograph and a permanent record of the test was obtained.

RESULTS

In all, 40 full-scale crash tests were conducted. The results were broken down into the primary results (the g values) and the peripheral questions which must also be answered before the yielding sign post can be considered as safe.

Primary Results

Table 1 gives the results of the field-testing program. Two criteria have been used for evaluating these results, the Stapp curve and the 10 g-50 msec criteria set by New York State. Great care must be taken in reporting results in this research area. Both peak values and average values of deceleration are often reported, but the exact definitions of these terms have never been spelled out. Note that both criteria for evaluating decelerations require both a g value and a time interval. For this program, decelerations were computed on the basis of distance traveled after impact. The curves from the photographic data were plotted in 2-ft increments after impact. This, of course, means more laborious computations, since a somewhat different time base is used for each test, depending on impact velocity. However, this type of computation enables each test to be compared to both of the standard criteria. Figure 9 shows a reproduction of the Stapp curves with the values of the peak decelerations superimposed. These peak values were computed for the first 2-ft increment of travel after impact. Figure 10 shows a similar curve with average deceleration values superimposed. In both Figures 9 and 10, tests which yielded a deceleration of less than 1.0 g are not recorded. These figures show quite clearly that no test of the yielding sign post exceeded either of the safety criteria.

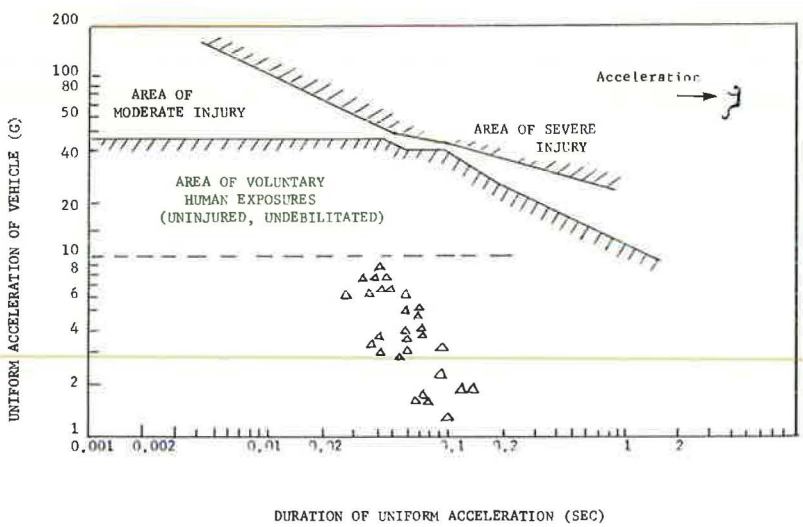

Figure 9. Peak values of deceleration.

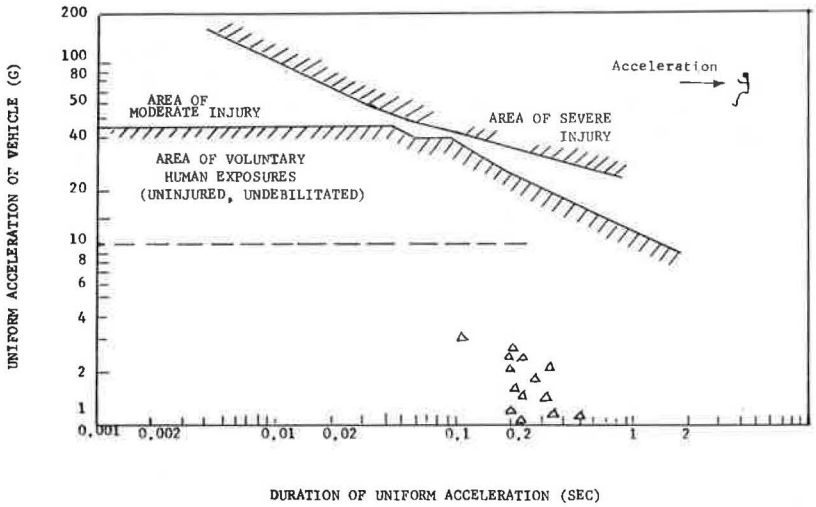

Figure 10. Average values of deceleration.

Secondary Results

In addition to the deceleration values, there are several peripheral questions which must be answered before the yielding sign supports can be considered safe:

1. Does the sign post actually yield as predicted?
2. Is there a reverse curvature of the post which would send the sign marker through the windshield?
3. Does the sign marker fly loose and become a hazard itself?
4. What effect do soil support conditions have on post behavior?

The 2-, 3-, and 4-lb sections, when struck by the automobile, yield at the ground line and the channel section spreads open. There is longitudinal splitting of the post along the bolt holes. At higher velocities (30 mph and up), the post may fail in tension after it has been flattened to the ground. The larger "piggyback" sections fail in a different fashion. These supports consist of two smaller sections bolted back to back (bolts at 16 in. center to center). Upon impact the post bends, thus shearing the bolts and permitting the sections to yield individually. During the crash test, every piggyback section failed as predicted. In the smaller posts, one test showed a shear failure at the bumper line. The rest of the tests showed good yield failures.

No sign marker caused serious damage to the windshield of the impacting vehicles. In only one test did the sign marker strike the windshield. In this one test, which was a double-posted installation struck at a 45-deg angle of incidence, the sign marker struck the windshield a glancing blow and cracked the windshield at the right lower corner. This is on the passenger side of the vehicle.

The flexible supports (2-lb and 3-lb sections) exhibited a reverse curvature when struck at higher velocities (30 mph and up). High-speed films show that the sign support yields at the ground line and bends forward, between the ground line and the bumper of the crash vehicle. Above the bumper line, the sign post, on first impact, bends back toward the vehicle. However, the momentum of the crash vehicle causes it to strike the post a second time and ride over the post, flattening it to the ground.

The method of attachment of the marker to the post naturally affects the behavior of the marker. In the early tests in the series, steel bolts were used to attach the sign marker to the post. Upon impact the steel bolts pulled through the sign marker, permitting the sign marker to fall. However, with the steel bolts there was a tendency for

the post to "throw" the sign marker. Most markers landed within 25 ft of the impact site, but one marker landed 40 ft from the point of impact. Midway through the test series, the switch was made to aluminum bolts. When the aluminum bolts were used, the bolts failed on impact and the sign markers fell quite close to the point of impact, generally within a 10-ft radius of the post.

Support conditions (driven post versus concrete) had only a minor effect on the yielding characteristics of the system. The actual crash test showed no appreciable difference in deceleration values between the driven posts and the posts set in concrete. Laboratory tests in a sand foundation showed that, for this type of foundation, both the post and the soil yield, permitting the vehicle to pass over with minimum deceleration.

CONCLUSIONS AND RECOMMENDATIONS

The field tests and the computer simulations clearly indicate that the 2-, 3-, 4-, 6-, and 8-lb steel sign supports currently used by the State of Ohio are yielding sign supports and may be considered safe to use.

The sign markers should be attached to the single-posted signs with aluminum, and not with steel, bolts. The aluminum clips used for the extruded aluminum sign markers on double-posted signs should be investigated further. These clips function well when the sign post is struck head-on or at a low angle of incidence. At high angles of incidence, these clips tend to slide along the sign marker and may present a safety hazard.

No tests were conducted on spliced posts in this research. Further research should be initiated to determine the safety characteristics of the spliced posts.

Both single- and double-posted signs were investigated in this program. No triple-posted signs were checked. These triple-posted signs should be the subject of further research.

REFERENCES

1. Rowan, N. J., et al. Impact Behavior of Sign Supports. Texas Transportation Institute, Summary Rept 68-2(S), Sept. 1965.
2. Edwards, T. C. Computer Simulation of a Breakaway Sign Support. Jour. of Highway Div., Proc. ASCE, Paper 5614, No. HW2, Nov. 1967.
3. Zaborowski, A. B. Human Tolerance to Lateral Impact With Lap Belt Only. Proc. 8th Stapp Car Crash Conf., Wayne State Univ. Press, Detroit, 1966.
4. Hodgson, V. R., et al. Response of the Facial Structure to Impact. Proc. 8th Stapp Car Crash Conf., Wayne State Univ. Press, Detroit, 1966.
5. Kroell, C. K., and Partick, L. M. A New Crash Simulator and Biomechanics Research Program. Proc. 8th Stapp Car Crash Conf., Wayne State Univ. Press, Detroit, 1966.
6. Nahum, A. M., et al. Injury in Non-Fatal Accidents. Proc. 8th Stapp Car Crash Conf., Wayne State Univ. Press, Detroit, 1966.